PRECIPITATE GENERATION AND CHARACTERIZATION OF CORROSION

SOURCE ALUMINA FOR GSI-191 CHEMICAL EFFECTS ISSUE

A Thesis

by

VIJAY RAVISANKAR

Submitted to the Office of Graduate and Professional Studies of
Texas A&M University
in partial fulfillment of the requirements for the degree of

MASTER OF SCIENCE

Chair of Committee,	Victor Ugaz
Committee Members,	Zhengdong Cheng
	Yassin Hassan
Head of Department,	Nazmul Karim

December 2016

Major Subject: Chemical Engineering

ABSTRACT

The release of corroded alumina during a Loss of Coolant Accident (LOCA) leads to deposition of these particles on the strainer, which consequently introduces a head loss that can cause shutdown of the cooling system. Salts of alumina have been used as surrogates for generating corrosion source particles to create a possible post-LOCA environment and for head loss testing. However, previous studies have shown that alumina surrogates tend to produce higher artificial head loss in the system compared to representative post-LOCA alumina particles, resulting in over-design of containment systems. It is therefore important to identify exactly what particles are generated, and relate their composition and properties to the corresponding head loss generated in order to develop more accurate predictions of LOCA scenarios. But surrogate formulations employed in head loss testing are likely not representative of actual corrosion products, making it difficult to assess the reliability of predictions based on these experiments. The goal of this study is to address the need for more pertinent data by exploring surrogate formulations produced from corrosion products obtained under chemical and thermal conditions mirroring those encountered during plant operation. The resulting precipitates are characterized physically and chemically using techniques including turbidity analysis, particle size distribution, SEM and to establish the influence of variables like pH and cooling rate. The resulting surrogates are then employed to assess head loss under LOCA conditions in a pilot-scale test facility. Our findings indicate that the quantity of aluminum corroded increased from 44 mg/L to 70 mg/L with an increase in pH from 7.2 to 7.5. The size of the particles increased with a decrease in cooling rate, with rapidly cooled particles having a diameter of

approximately 12 nm irrespective of pH, whereas intermediate and slow cooled particles increase in size with increasing pH. The results of these studies lay a foundation for development of improved surrogate formulations that can be used to obtain more accurate predictive capabilities to better mitigate LOCA events.

DEDICATION

To my dad, Ravisankar
To my mom, Lalitha Ravisankar
To my brother, Vivek Ravisankar
To my friends, Shalaka Burlawar, Adharsh Raghavan and Sathvik Divi

ACKNOWLEDGMENTS

I would like to thank my committee chair, Dr.Victor Ugaz, for his continuous support and guidance throughout the course of this research. I would also like to thank Dr. Zhengdong Cheng and Dr.Yassin Hassan for their support and accepting to be a part of my committee.

I would like to specially thank Chiranjivi Botre and Raja Ramanathan for continuous support and helping me during the course of my master's program. I would like to thank all my friends, colleagues, and the department faculty and staff for making my time at Texas A&M a great experience.

Finally, thanks to my parents and my brother for the support and encouragement

NOMENCLATURE

LOCA	Loss of Coolant Accident
RC	Rapid Cooling
IC	Intermediate Cooling
SC	Slow Cooling
ICP	Induced Coupled Plasma
NaTB	Sodium Tetraborate
TSP	Trisodium Phosphate
ECCS	Emergency Core Cooling System
SD	Shakedown
TEM	Transmission Electron Microscope
XRD	X-Ray Diffraction
CHLE	Corrosion/Head Loss Experiment
WCAP	Westinghouse Commercial Atomic Power
GSI	Generic Safety Issue

TABLE OF CONTENTS

LIST OF FIGURES

CHAPTER I

INTRODUCTION

The primary objective of the project is to perform in-situ corrosion of alumina to produce precipitate products that are representative of particles encountered in Loss of Coolant Accident (LOCA) scenarios. Corrosion of alumina results in the formation of insoluble chemical products under post-LOCA conditions and their resulting chemical effects directly impact Emergency Core Cooling System (ECCS) performance. A detailed physical and chemical characterization of the products is performed in order to establish the influence of parameters such as temperature and pH on the properties of the precipitates. These new results will help provide improved risk assessment and quantify the uncertainty of ECCS performance under a broad spectrum of LOCA conditions. The characterization studies will also help to guide preparation of new salt surrogate formulations for use in large scale strainer head loss tests with properties that more closely represent actual corrosion products

1.1 Background

General Safety Issue (GSI) 191 addresses the concern associated with generation of debris during a LOCA, their transport in the containment from the generation site to the sump strainers, and potential effects that such debris can cause to core cooling capabilities that may be affected by the amount of debris passing through the sump strainers. Chemical Effects Tests (CET) as a part of the GSI 191 resolution are broadly defined as any chemically induced phenomena that affect the performance of the ECCS. Initial chemical effects studies jointly sponsored by the US Nuclear Regulatory

Commission (NRC) and industry collaborators (Dallman et al., 2006) led to the Westinghouse Owners Group (WOG) study that provided a basis for deterministic quantification of chemical effects. An analysis of the WOG studies indicated a requirement of extreme measures to answer the GSI 191 issue and a more risk informed resolution would be beneficial and this could be done by enhanced characterization of the physical basis provided by the Westinghouse Commercial Atomic Power (WCAP) 16530 NP. (Lane et al., 2006) Extreme measures would require compliance with acceptance criteria for ECCS for light water power reactors through approved models and testing. This would result in extensive modifications and occupational dose and a more conservative approach through mitigative measures or use of South Texas Project (STP) approach may reduce the scope of modification and occupational dose (Borchardt, 2012) Specifically of interest to Texas A&M University are the generation and characterization of in-situ corrosion source alumina precipitates due to the presence of extensive alumina sources in the Palisades nuclear generating station located on Lake Michigan.

1.2 Deterministic Precipitate Study

A deterministic precipitate study was performed during WCAP 16530-NP testing and it was found that aluminum, silicon and calcium dominated the precipitate products formed. Sodium aluminum silicate ($NaAlSi_3O_8$) and aluminum oxyhydroxide ($AlOOH$) were thought to form in borated, sodium hydroxide ($NaOH$) buffered systems. Borated trisodium phosphate (TSP) was expected to support the formation of the former two along with the formation of calcium phosphate ($Ca_3(PO_4)_2$) as well. (Lane et al., 2006)

An initial study was performed by Los Alamos National Laboratory (LANL) to evaluate potential chemical effects occurring following a LOCA. The tests were performed with metal nitrates of aluminum, zinc and iron to cause precipitation and analyze the resulting head loss. The tests were however not performed in a typical post-LOCA environment with soluble salts used to generate metal ions for the formation of metal precipitates. (Johns, 2005) A more thorough study was done with joint sponsorship with NRC and Electric Power Research Institute (EPRI) to determine, characterize and quantify chemical products that may develop in the containment pool under representative conditions. (Andreychek, 2005) The results from these studies showed that the presence of sodium tetraborate facilitated corrosion of submerged alumina coupons leading to the formation of chemical precipitates that turn into gelatinous forms upon cooling.

Precipitates identified by the WCAP-16530-NP were in agreement with analysis done on ICET precipitates. (Dallman et al., 2006) (Klasky et al., 2006) WCAP didn't show any relation to precipitate generation with the total material released in solution. Release equations and precipitate stoichiometry were used to develop a model that quantifies generated precipitate mass. The aluminum release rates were determined with data from a number of tests, with the inclusion of ICET tests as well. Regression analysis performed on these data showed a dramatic increase in the aluminum concentration as pH was increased above 8. Salt surrogates were used to form these precipitate and a settling test was done prior to use in any GSI 191 resolution testing. (Lane et al., 2006)

Follow up studies found that WCAP produces non representative precipitates that may cause artificially high head loss. Bahn et al. (2011a) found that the chemically induced head loss from the salt precipitate was higher compared to the head loss from the corrosion source alumina precipitates. The testing concluded that there was an increased artificial head loss in case of AlOOH precipitate as compared to the head loss created from corrosion precipitates from a 6061/1100 alloy. This created a need of in-situ corroded particles that represent the particles formed under LOCA conditions to avoid the formation of any artificial head loss in the strainer so as to develop a more conservative approach to LOCA. (Bahn et al., 2009a) (Bahn et al., 2011a)

1.3 South Texas Project and Corrosion/Head Loss Experiment

The South Texas Project (STP) continued to increase the knowledge base of in-situ post-LOCA precipitate formation. STP's evaluation of representative post-LOCA precipitate was a product of their risk informed CET program. Precipitates obtained were either by slow salt addition or in-situ corrosion. Corrosion/Head Loss Experiment (CHLE) 010 effort provides results for the precipitate size difference and comparison of head loss response between the WCAP AlOOH surrogate and STP in-situ precipitate formed from slow addition of aluminum nitrate to a borated TSP buffer solution. (Howe, K. J., & Leavitt, J. J., 2012). The WCAP as mentioned previously was found to cause measureable head loss in both debris bed investigations. The in-situ corrosion particles were found to be 0.18 μm in diameter whereas the WCAP was around 1.6 μm. The corrosion particles were also found to produce considerably lesser head loss compared to the WCAP precipitates. CHLE 012 helped determine the quantity of aluminum corrosion reflective of median STP chemistry and exposed aluminum surface area and detect the

presence of chemical products that may form under the given conditions. (Leavitt, J. J., & Howe, K. J., 2012) CHLE 019 provides reference for size characteristics of typical precipitates formed from corrosion source materials exposed to representative post LOCA solution and the resulting chemically induced head loss of these precipitates. (Kim, S. J., & Howe, K. J.., 2013). Size analysis using zetasizer nano ZS showed evidence of particles less than 0.1 µm in diameter.

The increase in head loss due to in-situ precipitation of $Al(OH)_3$ seemed reasonably consistent with that expected from the addition of corresponding amounts of the WCAP surrogate. Per unit mass of Al removed from solution, the WCAP surrogate appears somewhat more effective in increasing head loss than the $AI(OH)_3$ precipitates formed in-situ by corrosion or chemical addition of Al, and thus it gives conservative estimates of the head loss due to the precipitation of a given amount of Al from solution. (Bahn et al. 2009c) Reasons for the difference in the quantity and the size between WCAP and in-situ corrosion are likely that the WCAP protocol ignored interdependencies between the pH, temperature, and the chemical constituents because the solubility parameters were not considered. In the current system, aluminum precipitates are of concern and previous testing showed aluminum precipitation in borated, NaOH buffered solution is predicted well by modelling amorphous $Al(OH)_3$, however little work has been done for the confirmation or identification of changes in behavior as a function of temperature or pH. (Bahn et al., 2011b) (Kim, S. J., & Howe, K. J.., 2013).

This chapter provided an introduction to GSI-191 and some basic studies that were performed to address this issue. Each nuclear facility performs its own resolution of GSI-191 issue by performing head loss tests using representative post-LOCA particles and use the results to determine a solution to the GSI-191. Generation and characterization of post-LOCA particles will help in performing head loss tests and also create new salt surrogates with properties similar to representative particles to be used in higher scale head loss testing. Next, in Chapter II, we review literature to provide an idea about the effects of operating variables on the particle characteristics and also the two main objectives of this project.

CHAPTER II

LITERATURE REVIEW

The purpose of the section is to provide references to discuss the key operating factors that affect the aluminum oxide precipitate formulation. Changing these variables during the bench or in-situ corrosion tests will influence the properties of generated precipitates such as morphology and size distribution.

2.1 Effect of pH

The effects of pH on resulting particle size and morphology of aluminum hydroxide/oxide have been demonstrated in a study using aluminum nitrate titrated with ammonia through a pH range of 3 to 8. (Zhou et al., 2012) A clear solution was formed with a pH < 3 and the precipitates changed from being flocculent to a thick white paste with an increase in pH. The visual observation obtained in this study indicated a strong influence of pH on stability, particle size and settling characteristics of aluminum hydroxide precipitates. Bahn et al (2009b) demonstrated this phenomena by showing that particle size increased as pH was increased from pH 7-8.5 and peaked at pH 9. Further increase in pH to 10 resulted in decrease in particle size measured. Though the $Al(OH)_3$ is a very representative compound, it has been found to undergo transitions in morphology with the change in the pH of the solution and therefore the representative post LOCA particles must be formed under the pH conditions that closely match the post LOCA conditions where precipitation is expected. The morphology and size of the particles were identified using TEM, ERD and Zeta Sizer analysis.

2.2 Effect of Temperature

Temperature also has an impact on the resulting precipitate particle size, phase formed, and morphology of the precipitates. In general, nucleation of precipitates has been found to occur rapidly at higher temperature and the smaller precipitates continue to grow at higher temperature. (Muschol, M., & Rosenberger, F., 1997). Cooling rates have also been found to affect the final precipitate morphology. (Chen et al., 2014) (Saito et al., 2012) Influence of cooling rates on various metal oxides found the effect of quick cooling (smaller particles) and fast cooling (larger particles)

With decreasing temperature or increasing cooling rates, the size of precipitates becomes finer and smaller. However a critical cooling rate usually exists beyond which the influence tends to become less significant. These were determined from other studies using coal slag and SnO precipitates generated by different cooling methods. The SnO precipitates were generated by natural cooling and by quenching using ice-water. The slow cooling rate reduced the number of crystal nuclei, and these nuclei grew large crystals. With the slower cooling, the SnO precipitates grew larger because the rate of crystal growth was greater than rate of nucleation. When the solution was cooled quickly, many crystal nuclei precipitated and formulated small crystals. (Saito et al., 2012) (Xuan et al., 2014)

The decomposition rate increases with the temperature because the formation and growth of nucleation occurs more quickly at higher temperatures. It was reported that ZnO crystals obtained are rod-shaped and become coarser at higher temperatures because the growth of crystals dominates the formation of nucleation at higher temperatures, leading to coarser crystals. Conversely, the nucleation prevails in the

process at lower temperatures, generating finer crystal (Chen et al., 2014). It was also found that the hydrothermal treatment at higher temperature promoted the crystallization and crystal growth. For example, the crystallite size will increase for CeO_2 coming from those hydrated $Ce(OH)_y(H_2O)_x(4-y)+$ or $CeO_2 \cdot n(H_2O)$ species before cooling down for precipitates, which is consistent with the dissolution precipitation mechanism. (Hirano, M. , & Kato,E., 1999)

For scale-up of reactions, reducing the overall thermal gradients in the reaction generated a more uniform product formation, while inhomogeneous effects and thermal gradients may be magnified severely during nanocrystal growth processes, resulting in poor nucleation and broadened size distributions. These effects have been noticed by synthesizing monodisperse nanoscale α-Fe_2O_3, InGaP, InP, and CdSe (Muschol, M., & Rosenberger, F., 1997) (Hu, X. L., & Yu J. C., 2008). Rational scale-up of laboratory-based protocols to the 50-100 gallon level is a critical objective of this project.

For scale-up reactions, reducing the overall thermal gradients in the reaction produced a more uniform product formation while inhomogeneous effects and thermal gradients may be magnified severely during nanocrystal growth process, resulting in poor nucleation and broadened size distributions. A NMR analysis was run on the AlOOH precipitates formed by the WCAP method (Leavitt, J. J., & Fullerton, C., 2013). Neglecting the interdependencies between the effects of pH and temperature , the particles generated were unrepresentative in nature and a worst case precipitate generation and ECCS performance evaluation was done based on these precipitates However, a risk informed approach evaluates representative conditions, precipitate

identity, representative morphology and behavior of precipitates to assess the probabilistic ECCS performance.

2.3 System Specific

The only containment materials that leach are calcium, aluminum and silicon. Since Palisades nuclear plantuses NaTB instead of TSP in containment, the possibility of calcium leaching can be ignored with a complete focus on effects of aluminum and silicon. In our system, the materials that leach or corrode aluminum into post-LOCA solutions are function of break type, therefore in a risk informed analysis, the maximum quantity of materials exposed to solution are variable. Worst case release of aluminum into the solution will be caused by the exposure summarized in table 1.

Table 1: Detailed table indicating worst case alumina release possible in Palisades plant

Submerged or Destroyed (both sides wetted)			
Aluminum Source	Thickness (in)	Surface Area (ft^2)	Weight (lb$_m$)
Paint	3.94E-04	56,297	156
Reactor Vessel Reflective Metal Insulation (RMI)	6.50E-04	30,344	139
RMI in the Bioshield Penetration and Large Break RMI	1.00E-03	40,660	286
Mineral Wool (Reactor and Pressurizer)	2.50E-03	3,132	55
Service Insulation (Aluminum Lagging)	1.60E-02	4,766	535
Large Break Mineral Wool (Corrugated Aluminum)	3.20E-02	1,578	355
Reactor Vessel Insulation Supports	1.25E-01	458	361
Reactor Cavity Insulation Supports	2.50E-01	264	440
Submerged Total		137,499	2327

Table 1 Continued

Sprayed (one side wetted)			
Aluminum Source	Thickness (in)	Surface Area (ft^2)	Weight (lb$_m$)
Pipe Covering	1.60E-02	12,420	2,809
Pressurizer Jacket (Corrugated)	3.20E-02	0	0
Light Fixtures	6.25E-02	700	600
Total Sprayed		13,120	3,409

2.4 Overview

A TAMU precipitate characterization test program was developed to characterize Palisades specific post-LOCA precipitates with two distinct objectives:

1. Consistent generation of representative particles under post-LOCA condition by corrosion of alumina foil

2. Characterizing the particles generated and identifying the effects of pH, cooling rate and the size and morphology of particles generated

The first step involves reproducible generation and preliminarily characterization of representative post-LOCA precipitates from corrosion sources for use in vertical head loss testing. This is followed by further characterization with uncertainties that may occur under the facility's specific conditions, with the ultimate goal of relating the morphology and type of precipitates to changes in cooling rate and pH.

Chapter II provided an insight about the effects of pH and temperature on the size and morphology of the particles and the two main objectives of the project. Consistent generation and preliminary characterization are major steps involved before head loss testing and provide the base for GSI-191 resolution. Next, in Chapter III, the facilities and the materials used to achieve the two objectives are explained step by step.

CHAPTER III

FACILITIES AND MATERIALS

3.1 Facilities

Two facilities were used for the testing conducted at TAMU. A bench facility consisted of a standard chemistry lab with general equipment to support bench testing. A tank facility consisted of corrosion tanks used to generate in-situ corrosion products, as shown in Fig 1. The corrosion tanks were chemically compatible with Palisades' post-LOCA solutions with a 100 gallon capacity and a maximum solution temperature of 85 $^{\circ}$C, pumps to allow vigorous circulation of solution across corrosion materials and smaller pumps to allow for transfer of in-situ precipitates to a vertical head loss loops. These tanks were also monitored using K-type thermocouples to ensure that temperatures were maintained within $\pm$ 2 $^{\circ}$C of the target value.

Figure 1: Corrosion tanks used to produce precipitates.

3.2. Materials and Methods

3.2.1 Materials

Boric acid and NaTB were obtained from vendors that supply nuclear grade materials. Aluminum metals obtained were alloy 1100 materials and were 1/16" thick 1' X 1' coupons (H-12) and 16-mil (H-14) thickness (foil).

3.2.2 Methods

Good laboratory practices were followed while conducting these experiments. Equipment and instruments used for measurements were calibrated continually during the experiments. The pH of the solution was verified to be within ± 0.1 before exposure to corrosion. Aluminum foils were rolled into three pieces and washed with DI water to remove solids and finger oils. Samples were stored in clean polypropylene containers, and samples for ICP testing were acidified using nitric acid at the time of collection.

3.3 Test Preparation

3.3.1 Water (DI H_2O) Preparation

A DI filter system was used to remove impurities before filling the corrosion tanks (Fig. 2). The DI water was run into a waste area until the TTS meter indicated a value less than 3 ppm. Once the system had been flushed, the tank was filled to the 50-gallon mark with water. Fig 3 shows the portable EUTECH Multiparameter PCSTestr 35 conductivity meter that was used to check conductivity. The conductivity was measured and verified if it was less than 10 µs/cm.

Figure 2: DI water filtration system

Figure 3: EUTECH Multiparameter PCSTestr 35 meter used to check water

3.3.2 Chemical Preparation

Boric acid and NATB were weighed on a lab scale and recorded in the lab notebook for review. Any chemicals used were from the same stock as the original 1 L bench-top test and massed on the same day to ensure that ambient conditions did not cause any changes in the molar mass of the reagents being used. The pH was matched to TAMU-Palisades test plan and the 1 L bench top solution after thoroughly mixing into the tank with a maximum error of $\pm$ 0.1. The boric acid and NATB were stored in airtight containers to prevent contamination.

3.3.3 Aluminum Foil Preparation

The required quantity of the specified aluminum foil alloy that matched the aluminum at Palisades was prepared before the test began. The outer layer of foil on the roll was removed and discarded. The required quantity of aluminum foil (estimated from

the required surface area) was massed into approximately three equal sheets. These sheets were loosely rolled ensuring a maximum exposure of the available surface area as shown in Figure 4. This ensured that the exposed surface area was maximized and that the target concentration of aluminum was reached in the calculated time.

Figure 4: Aluminum preparation before addition to corrosion tank.

3.3.4 Generic Test Procedure

This section reports the generic procedures applied to conduct the tests. Figure 5 shows the P&ID diagram for the corrosion tank system, depicting the equipment and instrumentation used to control the process:

1. The corrosion tank was filled with 50 gallons of DI water from the RO system, and the conductivity and turbidity were tested to ensure that they met the specifications listed under section 3.3.

2. Pump P-C1-1 was turned on and the chemicals were added to the tank to mix and fully dissolve. Once the chemicals were fully dissolved, the pH was recorded.

3. The heaters were turned on and the aluminum was added once the tank reached the target temperature. Once the foil was added, the test began.

4. After running for 4 hours, the pump was turned off, the aluminum removed from solution and the tank insulation was removed to facilitate cooling.

5. A sample was taken at the end of the 4-hour mark for ICP and was acidified with HNO_3.

6. Three samples were taken and placed directly into an ice bath for the rapid cooling. The temperature of these samples was monitored until they reached room temperature, after which they were removed from the bath.

7. Three samples were taken and placed into an oven that was set at 50 ^{0}C for 24 hours and was then turned off to generate slow cooled samples. The temperature of these samples was monitored during the cooling process.

8. After approximately 2 days, once the tank had cooled to room temperature, another three samples were taken to provide intermediate cooling rate data.

9. The size and turbidity of these samples was monitored over the next month to see if any significant changes occurred.
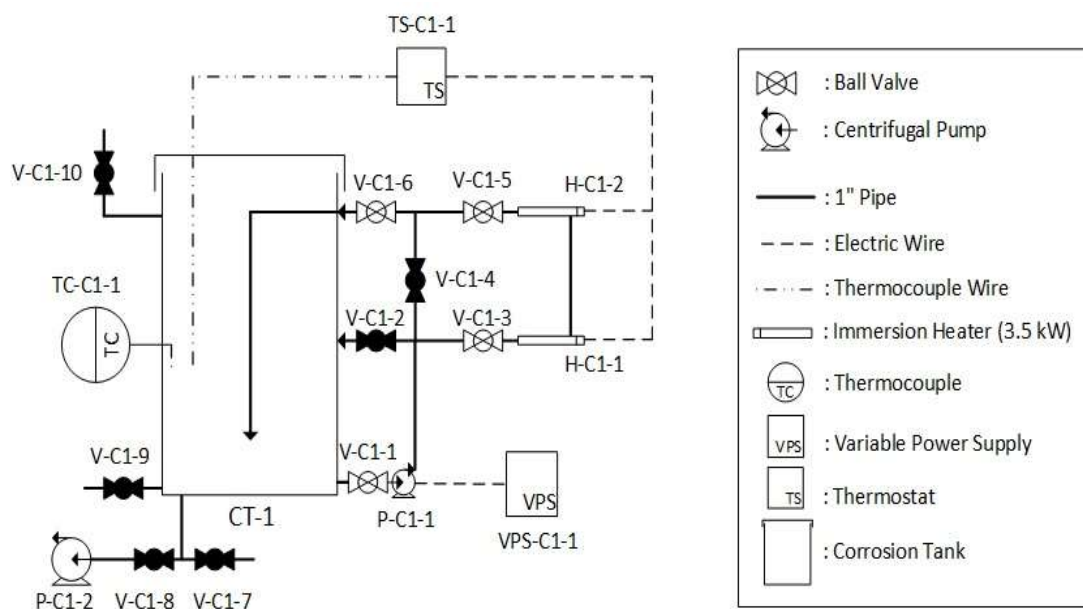
Figure 5: P&ID diagram of the tank structure used for up-scaled experimentation

3.3.5 ICP Analysis

A sample was taken at the end of the test and acidified with approximately 0.5 mL reagent grade 69% HNO_3 per 125 mL of sample to prevent any aluminum from precipitating out of solution before the ICP results were obtained. The instrument used to measure the samples was a Perkin Elmer NexIon 300D ICP Coupled Mass Spectrometer. The samples required dilution to be measured with the 300D ICP-S accurately since our range was above the upper detection limit of the machine.

Aluminum Standard (61935, FLUKA) for ICP (1000mg/L) was used to prepare the standards for the ICP analysis. Three standards were prepared within the range of 25-125 ppb by diluting the standard first with a spike solution and then with DI water. The spike solution was prepared by adding 7.3 g of boric acid to 500 mL of DI and then

adding 1.43 g of NATB to the same solution to obtain a buffer spike solution of pH = 7.2 at room temperature. The sample obtained from the corrosion test was assumed to have an approximate concentration of 50-100ppm and diluted accordingly with DI water alone so that it fell within the measurement range of the ICP instrument (2-200ppb)

The Perkin Elmer NexIon 300D ICP-MS instrument was used for the analysis. 1% nitric acid was used as the base matrix for the analysis. A daily performance check was performed to assess reliability of the equipment, and a 1% nitric acid solution was used as the blank solution for the analysis. A calibration curve was obtained from measurement of the standards prepared in the previous step. The values obtained from the ICP were compared with the values predicted from the dilution and the errors are compared to check the accuracy of the ICP-MS equipment. The aluminum concentration in the sample(s) were measured based on the calibration curve obtained from the standards. One of the standard was rechecked at the end to check any possible errors in the readings of the equipment after a certain period of run time.

3.3.6 Turbidity Analysis

Turbidity analysis included the turbidity results for any samples taken throughout the test. The samples taken were subjected to initial turbidity measurements as well as ongoing measurements over the next month to see if any change was observed. A HACH portable 2100Q Turbidimeter was calibrated with 4 NIST traceable formazin standards before measuring a sample's turbidity. The standards used were 10, 20, 100 and 800 NTU primary standards that enabled a repeatable and accurate calibration for measuring particles of various shapes and sizes due to the random variation in the formazin

polymer's length and folding structure. After the corrosion portion of the test was completed, the turbidity of the individual samples was measured. The turbidity was used as a base reference to determine if size was changing over time.

3.3.7 Particle Size Analysis

Initial particle size analysis was performed using a Nanoparticle Tracking Analysis (NTA) sizer, which uses the properties of both light scattering and Brownian motion to determine the size of the particles. However this analysis was found to be dependent on the dilution of the sample depending on the initial concentration, and was later replaced with a Zetasizer for more accurate measurements.

Particle Size Analysis is meant to classify the particles by size. DLS was used to measure the particles suspended in solution. The Brownian motion of the particles causes the incident laser light to be scattered at various intensities. The collector is then able to analyze this data and with the Stokes-Einstein relation. This relation holds true for spherical particles suspended in aqueous media exhibiting a low Reynolds number.

To analyze the samples taken from the 3000 series test, we used a Malvern Zen 3600. The instrument was calibrated with NIST traceable 60 nm and 100 nm standards. The method is described in detail below and summarized in Table 2

Polystyrene Microsphere Standards

The 60 and 100 nm standards were prepared in approximately a 1:30 dilution (or 1 drop of standard in 1.5mL of Nanopure DI water) run through the machine before any batch of samples to confirm that the instrument is reading correctly and properly

calibrated. Table 2 describes the results obtained from the instrument. The error given by these readings fell within an acceptable range for the instrument and standard.

Table 2: Polystyrene microsphere standards used for calibration

Standard	Catalog Number	Description	Mean Diameter	%RSD $(\sigma/\mu)*100$
Duke Scientific 60 nm Microsphere	3060A	Polymer microspheres in water	60nm (+/- 2.5nm)	16.8%
Thermo Scientific 100 nm Nanosphere	3100A	Polymer microspheres in water	100nm (+/-3nm)	7.8%

The results from the NIST standards on the Zen 3000 are presented in the Fig 6 and Fig 7 and summarized in Table 3 below.
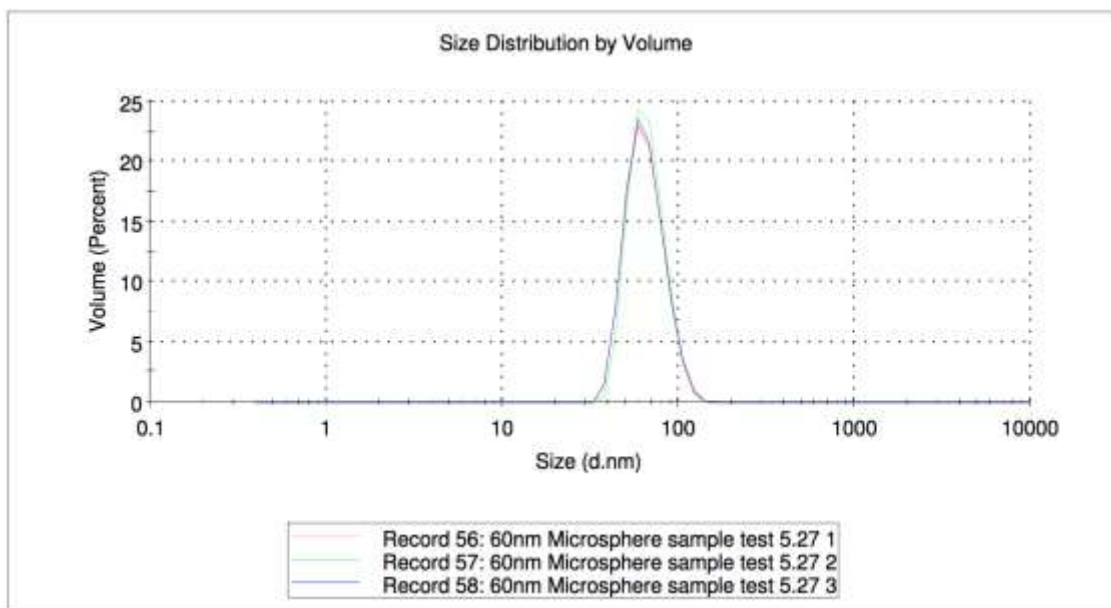
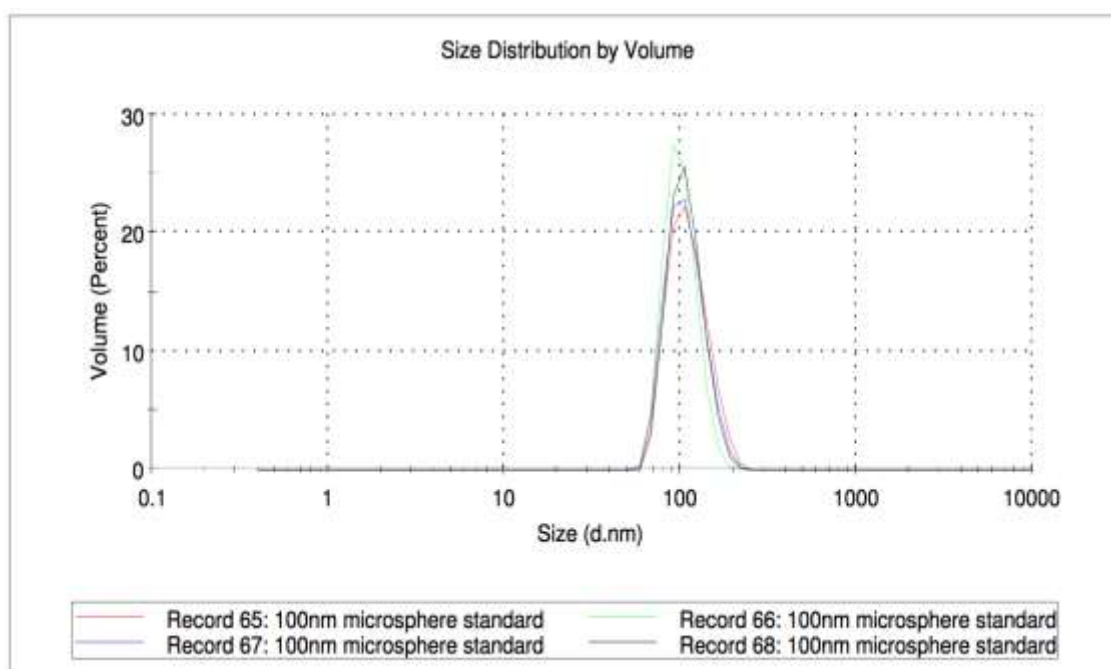Figure 6: Size distribution for three independent runs of the 60 nm microsphere standard.

Figure 7: Size distribution for 4 independent runs of the 100 nm standard.

Fig 6 and Fig 7 represent the size distribution for multiple independent runs of the 60 nm polystyrene microsphere standard and the 100 nm standard through the Malvern nanosizer. The distribution of the particles fell within the expected range for the instrument's limitation as well as for the expected variation in the polystyrene standards.

Table 3: Particle standard size summary

Sample	Size (nm)	Standard Dev (nm)	Polydispersity Index(Pdi)
60 nm Standard	65.67	16.36	0.007
100 nm Standard	108.7	24.73	0.076

3.3.8 Experiment Timeline

Each experiment took approximately four days to complete, which included running the experiment followed by analysis on the collected samples (Fig 8). The first step involved cleaning of the tank with washes using DI water which were repeated until the electrical conductivity (EC) of the liquid in the tank fell below 10 μS/cm. The DI water used to wash the system was run into a waste area until the TDS meter indicated a value less than 3 ppm. The tank was filled with 50 gallons of water once both the TDS and EC were below the respective values. The filling of the tank took about an hour during which time the chemicals and aluminum foil required were then weighed on lab balance scale . The chemicals were added into the DI water and the solution was then heated to 85 °C using the heaters in the system. It took approximately 3 hours to reach the target temperature. The foil was added into the solution and incubated for corrosion

for the next 4 hours. A sample was collected and acidified with nitric acid for ICP testing. Three more samples were taken and placed in an ice bath and allowed to cool for around 30 min until samples reached room temperature. Three additional samples were acquired simultaneously and placed in an oven at 50 °C and placed at constant temperature for a day, after which they allowed to cool down to room temperature, taking about 2 days in total. While taking samples for rapid and slow cooling, the insulation around the tank was removed allowing the tank to cool down in ambient surroundings. The samples after cooling were analyzed to determine turbidity and particle size distribution of the precipitates in the solution. The samples collected for ICP testing were then analyzed to determine concentration. These combined tests took about 4-6 hours, including the time for sample and standard preparation.
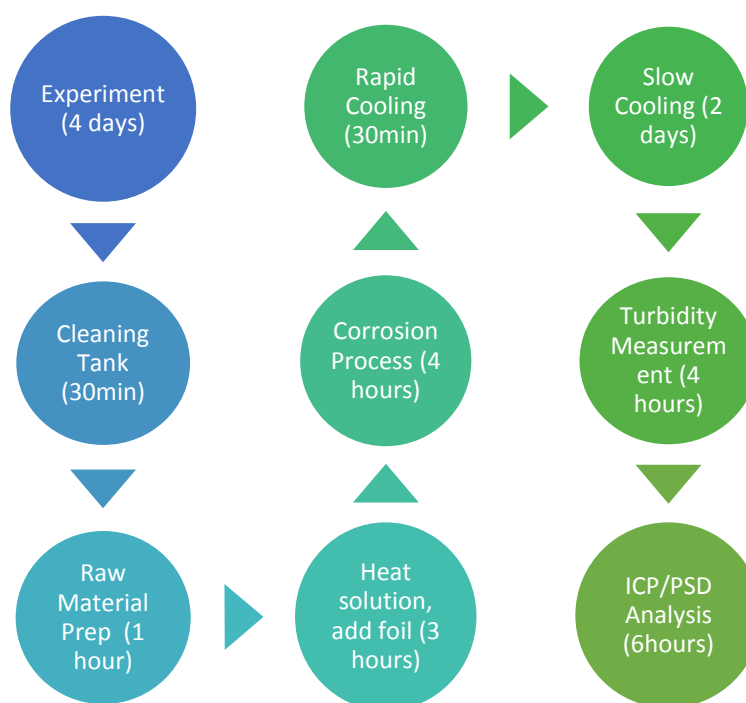

Figure 8: Flowchart describing the typical experiment timeline.

Chapter III provided a detailed step by step procedure used to achieve the two objectives mentioned in Chapter II. The facilities and materials used and the various analysis methods used helped in consistent generation of particles followed by the characterization of the same. Next, in Chapter IV, the test plan used to achieve the objectives and the effects of pH and cooling rate on the size and morphology of the generated particles.

CHAPTER IV

RESULTS AND DISCUSSIONS

This section is divided into two parts. The first part describes the consistent generation of in-situ corrosion source alumina precipitates that produced at least 10.6 g of aluminum as required by the TAMU facility. The second part reports preliminary characterization of the alumina precipitates, and effects of pH and cooling rate on the size and morphology of the particles produced.

4.1 Test Plan

The first part of the test plan consisted of bench experiments to generate and characterize AlOOH particles from borate buffer solution at pH 7.2. This was followed by another set of bench experiments to generate alumina precipitates by corrosion of alumina foil at two different pH. The process was then up scaled to a 50 gallon level and shakedown experiments were performed to optimize the quantity of alumina foil and corrosion time needed to achieve the target concentration of alumina precipitates. The optimized process was then used to perform in-situ corrosion of alumina over range of different pH, followed by cooling the corrosion products at three different cooling rates. The effect of pH and cooling rate on the particle size distribution, morphology and turbidity was then analyzed.

4.1.1 Summary and Goal

One objective of the Palisades precipitate characterization testing at Texas A&M was developing a procedure to form in-situ aluminum precipitates with repeatable size

characteristics (D50 of 150 nm) for use in head loss testing. There was also a requirement that the corrosion tank must produce 10.6 g of corroded, soluble alumina within the palisades specific chemistry bounds. This goal was to be attained prior to start of head loss testing. It is important that the corrosion source alumina produced the superficial loading limit required by our system as mentioned in Table 4.

Table 4: Superficial loading limits in the current plant system.

Facility	Mass of aluminum released	Strainer area	Superficial loading (L*)
Palisades	190.2 kg	327.39 m^2	581 g/m^2
TAMU	10.6 g	0.0182 m^2	

The corrosion procedure was performed at Large Break LOCA (LBLOCA) at pH = 7.2, at Small Break LOCA (SBLOCA) at pH = 7.5, and also at pH = 8.2.
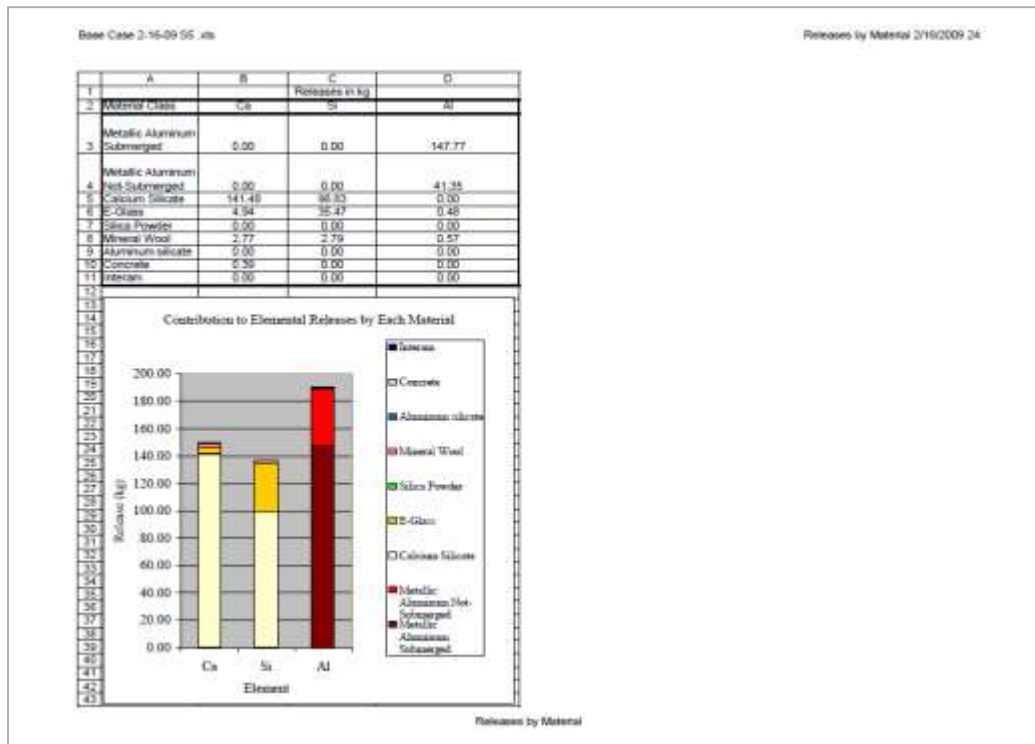
Figure 9: Total amount of chemicals released after corrosion in the current plant system.

The amount of aluminum released in case of LOCA can be determined from figure 9. We determine a 190.2 kg release of aluminum for the plant with the strainer size of 327.29 m^2. The superficial loading can be calculated to be 581 g/m^2. With the strainer size of 0.0182m^2 in the TAMU facility, our aim is to achieve an equal superficial loading and therefore require at least 10.6 g of aluminum produced in the corrosion tank.

4.2 WCAP Formulation Protocol
4.2.1 Description of Tests

The goal of these tests was to familiarize with the WCAP protocol for use in head loss testing. The AlOOH synthesis recipe was based on WCAP-16530 (Lane et al., 2006). The formulated solutions were produced at 2 different concentrations of 2.1 and

11 g/L. The prepared precipitates were cooled from 80 °C to room temperature and poured into bottle to sediment. The settled precipitates were then used to prepare SEM samples. This procedure was repeated but scaled up recipe to produce 10 bottles of 10 g/L precipitates. The total amount of 100 g AlOOH precipitates were formulated also to support head loss testing. The formulated AlOOH from the bench scale all passed the sedimentation test specified in the WCAP 16530 (6.5 mL out of 10 mL sample in 1 hour)

4.2.2 Analysis and Results

Table 5 shows formulated precipitates at concentrations of 2.1 g/L and 11 g/L. The recipes are scaled from WCAP 16530. The appearance of precipitates is pictured from top view of the reactor. The SEM images were captured by using extracted and dried samples.

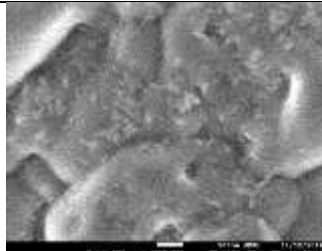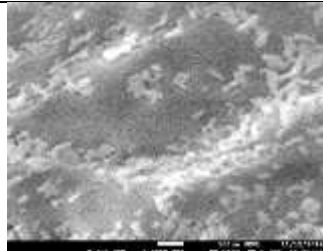Table 5: Bench corrosion tests producing different concentrations of precipitates.

Precipitate formation and concentration	2.1 g/L AlOOH	11 g/L AlOOH
Water in pot (L)	0.2	0.2
$Al(NO_3)_3 \cdot H_2O$ (g)	2.62	13.76
NaOH (g)	0.84	4.36
Temperature (ºC)	80	80
Picture for solution, top view of the reactors at 80 °C showing turbidity of the respective solutions		

Table 5 Continued

Precipitate formation and concentration	2.1 g/L AlOOH	11 g/L AlOOH
SEM images of dried flocculation		

The reagents used to produce a scaled up total of 100 g AlOOH precipitates for HL tests are listed in table 6. The recipe is scaled according to the WCAP 16530 NP. Surrogate salts were added into the 1 L volume in the reactor and stirred for 10 min.

Table 6: Detailed quantities of materials used for AlOOH precipitate preparation.

#	Al(NO$_3$)$_3$·9H$_2$O/g	NaOH/g
1	62.53	20.03
2	62.55	20.03
3	62.46	20.00
4	62.48	19.99
5	62.49	19.99
6	62.50	19.99
7	62.48	19.99
8	62.47	10.04
9	62.53	19.99
10	62.49	19.97

4.2.3 Conclusion

Formulation of AlOOH was successfully completed based on WCAP procedure. The solution with higher concentration was more turbid as seen from the images table 5.

The formulation was to practice the creation of solution for head loss testing with the required amount of concentration and recreate the WCAP procedure. The SEM images do not provide optimal view of individual precipitate particles because samples were not calcined before testing. The next step would be performing bench scale corrosion of aluminum foil to generate a more representative post LOCA product instead of one generated using salt surrogates.

4.3 Aluminum Corrosion in Bench Tests

4.3.1 Description of Tests and Generic Procedures

Two corrosion tests were performed to examine release of Al into the Borax/Boric Acid solution by aluminum foil corrosion under representative palisades post LOCA conditions. The purpose of the first bench corrosion test was to release Al from foil in the borax/boric acid solution prepared referring to the palisades post-LOCA conditions. The purpose of the next bench test was to adjust pH of solution by using aqueous NaOH solution and to release Al from foil at a higher pH solution.

4.3.2 Analysis and Results

Table 7a and 7b show the pH and temperature readings at different steps during the bench tests.

Table 7a: pH and temperature variations during bench test 1.

Test step for Bench Test 1	Accumulated NaOH	1		2		3	
		pH	Temperature/°C	pH	Temperature/°C	pH	Temperature/°C
Heated Solution upto 85⁰C	0	7.24	85.5	7.23	86.6	7.25	85.6
After Corrosion	0	7.2	82.7	7.18	85.2	7.17	86

Table 7b: pH and temperature variations with variation in input raw materials concentrations during bench test 2.

Test step for Bench Test 2	Accumulated NaOH	1		2		3	
		pH	Temperature/°C	pH	Temperature/°C	pH	Temperature/°C
Original	0	7.33	21.6	7.32	21.9	7.34	21.7
Added 1.0 g 0.01 mol/L NaOH	1.0 g 0.01 mol/L NaOH	7.35	21.7	7.34	22.6	7.35	22
Added 9.0 g more 0.01 mol/L NaOH	10 g 0.01 mol/L NaOH	7.37	20.8	7.36	21.2	7.37	20.5
Added 90 g more 0.01 mol/L NaOH	100 g 0.01 mol/L NaOH	7.44	21	7.43	21	7.45	21.2
Heated solution up to 85°C	100 g 0.01 mol/L NaOH	7.34	81.4	7.35	81.2	7.33	82.5

Table 7b Continued

Test step for Bench Test 2	Accumulated NaOH	l		2		3	
		pH	Temperature/°C	pH	Temperature/°C	pH	Temperature/°C
Added 100 g more 0.01 mol/L NaOH	200 g 0.01 mol/L NaOH	7.40	82.8	7.41	82	7.40	83
After corrosion	200 g 0.01 mol/L NaOH	7.31	82.6	7.32	82	7.32	82

The final appearance of the aluminum foil samples after corrosion is shown in figure 10. A more pronounced dark layer on the surface of foil for bench test 2 was observed. During bench test 2, a higher surface of Al foil and higher pH solution for corrosion was used.

(a)   (b)

Figure 10: Corroded alumina foil from bench corrosion tests a) Bench Test 1 b) Bench Test 2

4.3.3 Conclusion

During the bench corrosion test 1, the release Al by corrosion in the bench reactor was 30 mg/L into original borax and boric acid solution. The value matched with later Al released into scale up in-situ corrosion tank test (section 4.4.1 Fig 11). The solution was adjusted for pH in the next test and the corrosion was found to be higher, about 44 mg/L. The work provides preliminary corrosion data for the Al release in the solution compatible with post-LOCA. The amount of Al foil used is calculated based on scaling of actual conditions in Palisades specific post-LOCA scenario.

4.4 Shakedown Tests

Four tests using the corrosion tanks of the tank facility were conducted and each test was performed with specified amounts of boric acid and NaTB decahydrate which is expected to produce a solution of the required pH at 21 °C. The solution was heated to 85 °C and aluminum foil was submerged to allow corrosion. The mass and estimated surface area of aluminum exposed in shakedown tests 1-4 are summarized in table 8, along with the released mass and resulting D_{50} PSD as seen in figure 11 and figure 14 respectively.

Table 8: Mass and surface area of alumina foil added during different shakedown tests.

Aluminum Foil	SD 1	SD 2	SD3	SD4
Surface Area (m^2)	0.28	0.29	1.13	0.58
Mass (g)	15.20	15.48	60.80	30.40

4.4.1 Analysis and Results

Aluminum Release as a Function of Corrosion Time

The fluid samples collected from the corrosion tank were further diluted 1% HNO_3 to the concentration ranging from 2-200 ppb and ICP-MS measurements were performed according to the following procedure. The target concentration of 56 mg/L (10.6 g for 50 gallon tank) was established in a memo provided by the company. Al concentration did not reach saturation because the test did not run for enough time. The Al concentration in SD-2 reached the saturated concentration of 50 mg/L which is quite close to the target value. In order to increase the saturated concentration of Al, the surface area of the Al foil was increased. However it was found that Al concentration quickly increased in the beginning and then decreased when extending the corrosion time beyond the point where this saturation is reached. The chemistry can be manipulated to attain the desired aluminum corrosion by increasing the pH of the bulk solution or increasing temperature. Since there was a limit on the equipment capabilities and a limit of 85 °C for running the equipment, the pH of the solution was increased from 7.2 to 7.5 and a higher saturated concentration of 70 mg/L was successfully achieved. Comparing these results, it can be concluded that increased pH will help to enhance the Al released from the foil, which is applicable to reach the target Al concentration in the corrosion tank.
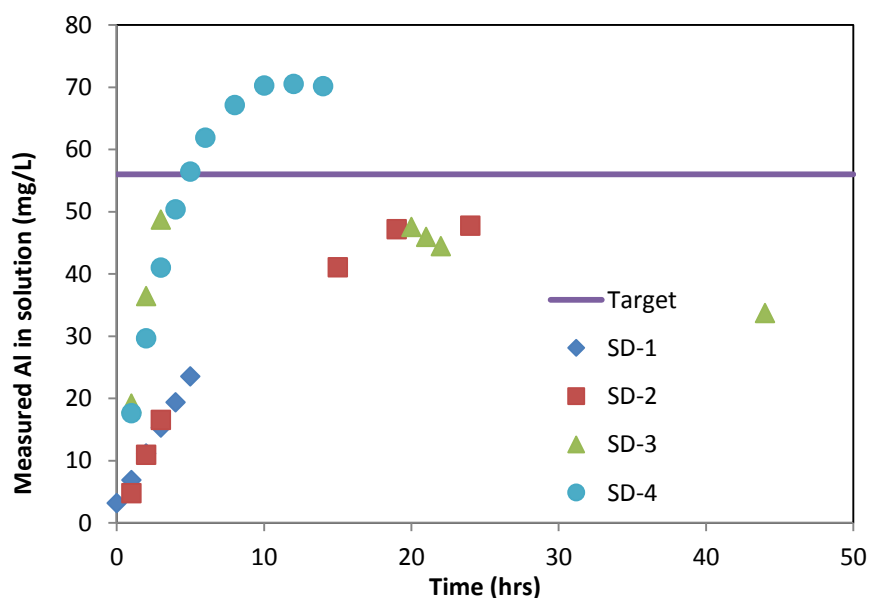
Figure 11: Aluminum concentration at different times during shakedown tests.

Solution and Foil Appearance

The appearance of the generated precipitates became more and more turbid. Especially in SD-3, the largest surface area of Al foil and the longest corrosion time were used to generate the most turbid precipitates (Fig 12a-d). A dark passive layer on the surface of the removed Al foil could be observed in SD-2,3,4 as seen in Fig 13a-d. Moreover, considerable white deposits could be observed on the surface of the removed SD-3 corroded foil. These white deposits came from the suspension and accumulated on the foil surface, which consequently decreased the Al concentration when extending the corrosion time beyond the point where this saturation is reached in SD-3 is shown.

a

b

c

d
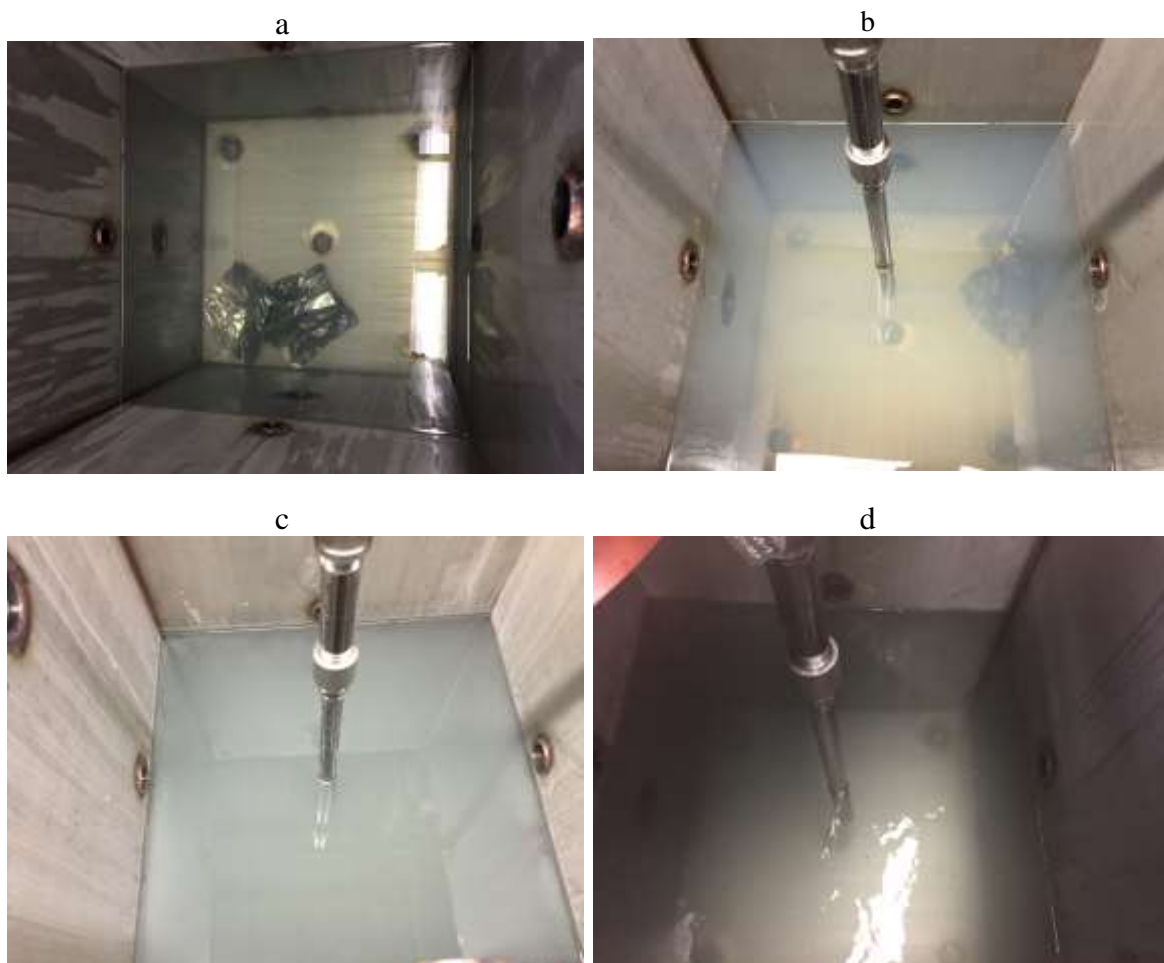
*The top view geometry of the tank is 61 cm x 61 cm

Figure 12: Suspension appearance after each corrosion test: a) SD-1; b)SD-2; c)SD-3; d) SD-4.
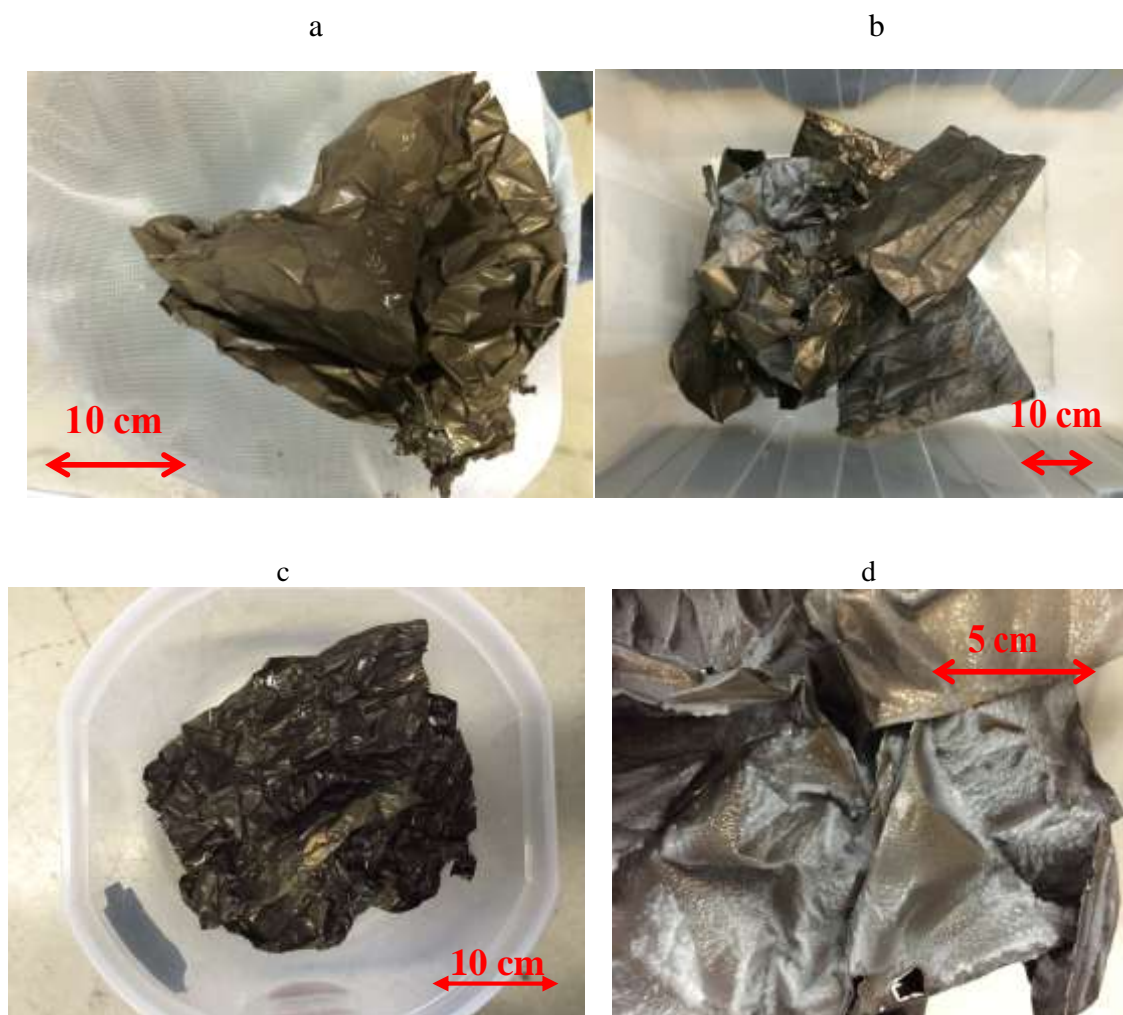
Figure 13: Foil appearance after corrosion test: a)SD-1; b) SD-2 and c) SD-3; d) SD-4.

Particle Size Distribution

NTA was used to characterize 100 nm size standards over a range of different dilutions. These data indicate that diluted samples shift to larger size ranges. The dilution factor is dependent on the concentration of the samples collected from the corrosion tank. 100x is the best possible dilution for the samples, and particle size distributions were determined using this value (Fig 14).

a

b

Mean 201.06 ± 68.48 nm

Median 191 nm

Mean 164.15 ± 59.9 nm

Median 155 nm

c

d

Mean 233.69 ± 82.18 nm

Median 223 nm

Mean 186.84 ± 63.72 nm

Median 176 nm
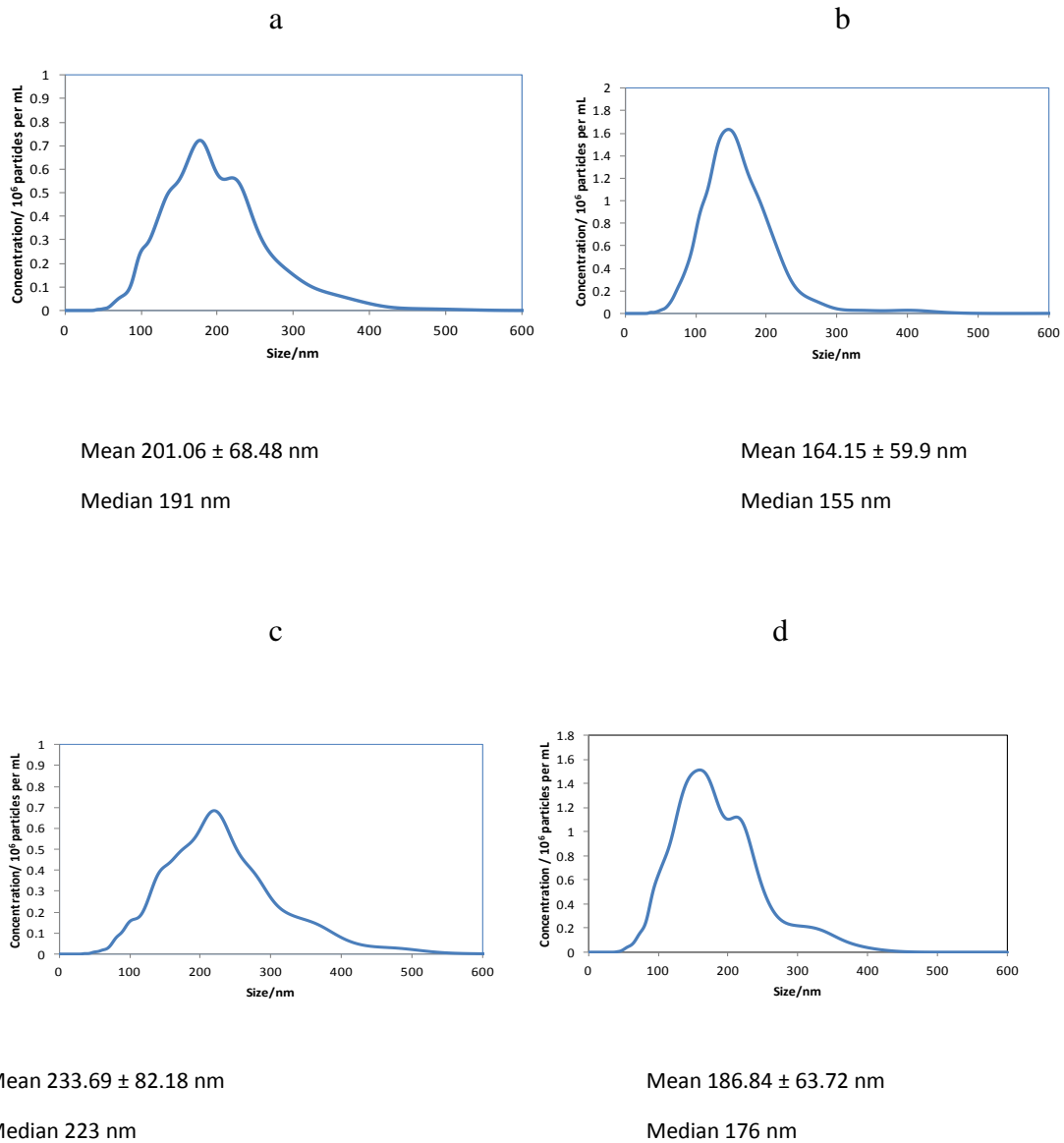
Figure 14: Particle size distribution Analysis from the different shakedown tests a)SD-1;

b) SD-2 and c) SD-3; d) SD-4

Cooling Rate

The temperature inside the corrosion tank was measured by K-type thermocouple and recorded by LABVIEW. The thermocouple was placed close to the bottom of the suspension in the tank. The cooling rate for each test is shown in Figure 15. In SD-4, we manipulated the condition as SD-2 and successfully obtain the similar cooling rate.
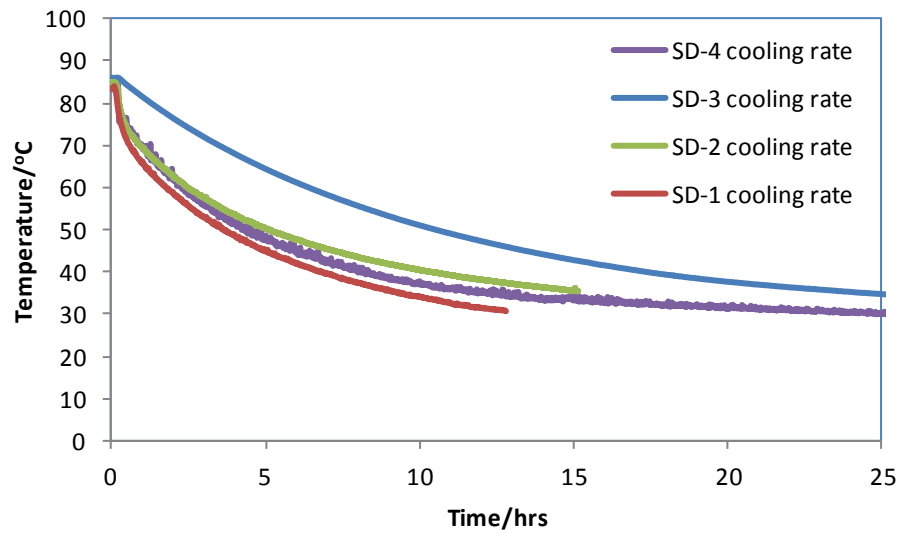
Figure 15: Cooling rate analysis from shakedown tests.

Turbidity

Turbidity was measured using a HACH 2100Q portable turbidimeter. Samples were stored for 1-2 weeks and the measurements were done at room temperature. It was clearly observed that the turbidity of the samples increased with the Al concentration. It is seen that, even though final three samples collected for SD-4 have almost same concentration (Section 4.4.1, Fig 11), their turbidity keeps increasing with the corrosion

time. The inference was supported by the fact that the final sample had a higher turbidity but with decreased Al concentration measured by the ICP.

4.4.2 Conclusion

The corrosion rate is related to the initial surface area of Al foil. Higher surface of Al foil will lead to a faster corrosion rate in the beginning of the test. With increasing corrosion time, the Al in solution reached saturation at around 50 mg/L in SD-1,2,3 and 70 mg/L in SD-4 which was performed at a higher pH of 7.5. Extending the corrosion time beyond the point where this saturation is reached will cause white deposits to form on the surface of the Al foil and consequently reduce the solid concentration in the suspension. This will also introduce difficulties to correlate the solution turbidity to the precipitate content, as discussed below.

The size of the final precipitate for each in-situ corrosion test ranges from 60-200 nm . The PSD from the NTA measurement is dependent on the dilution of the sample. Usually, diluted samples give shift to the higher size range. The appropriate dilution is dependent on the concentration of the samples we collected from the corrosion tank. Regarding the concentration range from our shake down tests (~50 mg/L Al), 100x dilution is recommended.

The cooling rate was manipulated in different method in each in-situ corrosion tank SD test. The pumping pipeline was modified in SD-2, which caused a difference in cooling rate between SD-1 and SD-2. During the cooling procedure in SD-3, we kept the insulator on the pumping pipeline, which slowed the cooling rate. These operations will be considered to determine the optimal way to control the cooling rate in future tests.

Finally, in SD-4, we repeated the manipulation as SD-2 and reproduced the similar cooling rate.

Turbidity increases with concentration of Al, and also increases with corrosion time. To correlate the turbidity to the Al released in the corrosion solution, the corrosion time should be introduced as a correction term to ensure that the turbidity correlation more accurately reflects the elemental concentration so that the solid precipitate content in solution can be correctly estimated.

4.5 In-Situ Tests
4.5.1 Introduction and Scope

Tests were performed to generate and characterize corrosion source aluminum precipitates formed under facility's post-LOCA conditions. The tests were performed using the corrosion tanks where Al was produced under specific conditions described in the test plan. Precipitation of Al was induced by cooling the solution to room temperature with different cooling rates. The aim is to generate and characterize representative in-situ aluminum precipitates and observe how changes in the pH and cooling rate affect particle characteristics of aluminum hydroxide/oxide, such as particle size and morphology.

4.5.2 Test Conditions

Temperature

The temperature of the corrosion tank solution was maintained at 85 ± 2 °C. The temperature may be elevated up to 2 °C before aluminum addition to ensure the temperature is within range at the test start and does not drop below when the lid is

removed for the foil addition. To induce precipitation, solution was cooled to room temperature with different cooling rates.

Cooling Rates

Three different cooling rates were imposed during the tests, as specified earlier. A fast cooling rate was achieved by immersing the Al solution samples into an ice bath. Intermediate cooling was achieved by cooling the solution in tank by natural circulation, after removing the insulation panel. A slow cooling rate was established by controlling temperature of solution sample in a lab oven.

System pH

The pH of the system was kept at 3 different conditions of 7.2, 7.5, and 8.2 The pH was varied by changing the quantities of boric acid and NATB added to the solution and the solution pH was checked to be within an error of ± 0.1 before the start of corrosion.

4.5.3 Results and Discussion

3101/3201

Tests 3101/3201 were completed. Samples were exposed to three different cooling rate and the PSD and turbidity of the samples were analyzed. The scope to investigate the combined effect of pH and cooling rate (Table 9) on aluminum precipitate characteristics. The effect of pH was assessed by comparing the results of the current test with the 3102/3202 tests and 3102/3203 tests.

Cooling Rates

Table 9: Cooling rate data for test series 3101/3201.

Sample description	Cooling rate (degrees C/minute)	Total cooling time (minutes)
Rapid Cooled sample (RC)	Figure 16	21.5
Tank Cooled sample (TC)	Figure 16	2,384
Oven Cooled sample (OC)	Figure 16	2,880
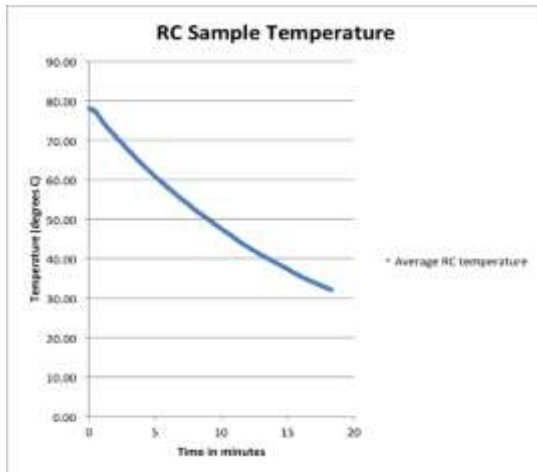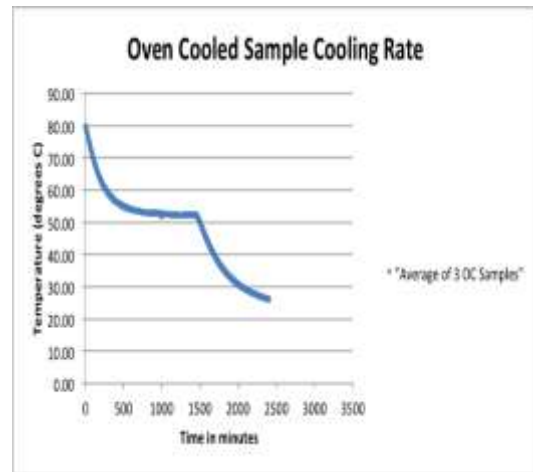
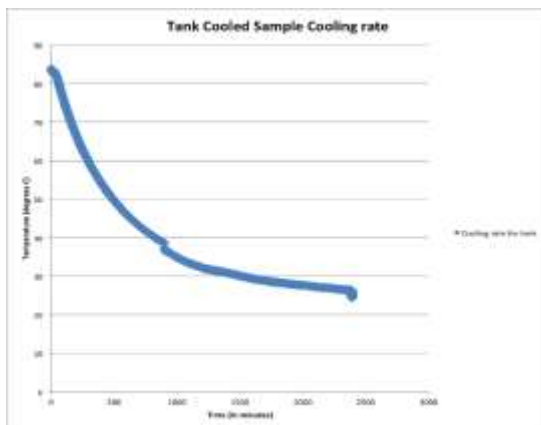(a)   (b)

Figure 16: Cooling rate graphs for tests series 3101/3201 (a) Rapid Cooling (b) Slow

Cooling (c) Intermediate Cooling

(c)

Figure 16 Continued.

ICP Analysis

The Perkin Elmer NexIon 300D ICP-MS equipment was used for the analysis. 1% nitric acid was used as the base matrix for the analysis. A daily performance check was performed on the equipment before the analysis to check the reliability of the equipment and a 1% nitric acid solution was used as the blank solution for the analysis. A calibration curve was obtained from the measurement of the standards prepared in the previous step. The values obtained from the ICP were compared with the values predicted from the dilution and the errors compared to check the accuracy of the ICP-MS equipment. Table 10 shows the aluminum concentration in the sample(s) that was measured based on the calibration curve obtained from the standards. One of the standards was checked again after the sample to check any possible error in the readings of the equipment after a certain period of run time.

46

Table 10: Concentration analysis for test series 3101/3201

Sample name:	Concentration (mg of Al per Liter)	Standard Deviation (mg/L)	% RSD
Sample 1	47.77	1.97	4.09%
Sample 2	48.46	1.91	3.97%
Average	**48.12**	**1.94**	

Turbidity Results
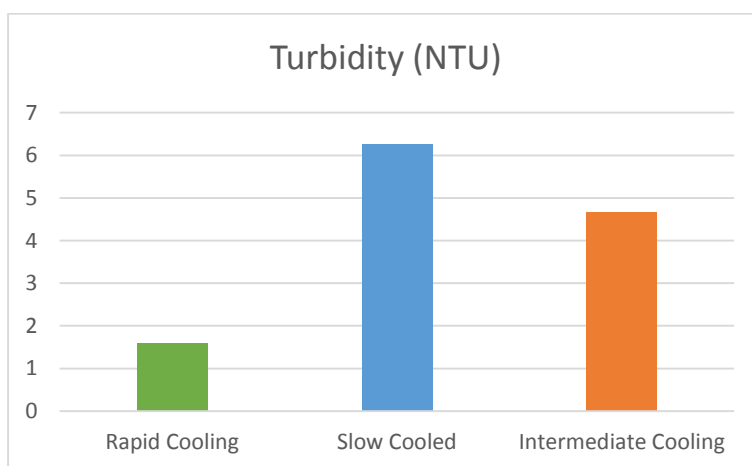
Figure 17: Turbidity analysis for test series 3101/3201.

The cooling rate data display a trend of larger particle size and higher turbidity for the samples with a longer cooling time (Fig 17). The cooling duration for a given sample has a direct correlation to the particle formation and overall precipitate size. Continuing to monitor any changes in turbidity over time will allow us to determine of

future size measurements are required or if there is any change to the precipitate size or morphology after cooling has completed.

Particle Size

Table 11: Particle size distribution analysis for test series 3101/3201,

Sample Name	Size 1 (nm)	Volume percent of size 1	Standard Deviation (nm)	Size 2	Volume percent of size 2	Standard Deviation (nm)
TC	32.64	85.2%	16.59	5180	12.4%	764.5
QC	13.2	99.4%	2.46			
OC	42.67	82.7%	21.72	5244	14.9%	732.3

Table 11 shows the results on particle size distribution at different cooling rates. The quick cooled samples have a slightly larger variation in size than the tank cooled samples, which is due to the variation in position in the ice bath. This resulted in slightly different cooling rates and a larger standard deviation in the particle sizes than the TC samples.

TEM Images

Analysis of three samples using the three cooling rates (RC, IC, and SC) were performed with TEM to study precipitate characteristics of interest such as morphology and composition. Different areas were subject to observation and analysis from the samples selected. Figures 18, 19, and 20 summarize the main observations for selected

areas of the RC, IC, and SC samples respectively. Samples showed aluminum-compound particles of various size, morphology, composition, and crystallography. Graphitic particles and sodium-containing aluminum compounds were also detected (copper and carbon come mainly from the TEM grid).

The analysis conducted on the RC sample showed amorphous Al compound with the intensity Al/O ratio of ~ 0.5 (Figure 18). In Figure 19 (IC sample, Area 2) a large particle on a micrometer scale is seen and indexed as a single crystal by the selected-area diffraction pattern. Its surface is at least partially porous. Though particles observed in RC and IC are different in morphology and crystallography they show similar compositional properties. A different area for the IC sample show crystallinity but have different composition than the other samples. The EDS intensity ratio is around 2. Surface of the particles appears very smooth. Along the surface of large particles and the edge of holy carbon film there are some small particles, which might be the same with the particles seen in the RC sample.

(a)
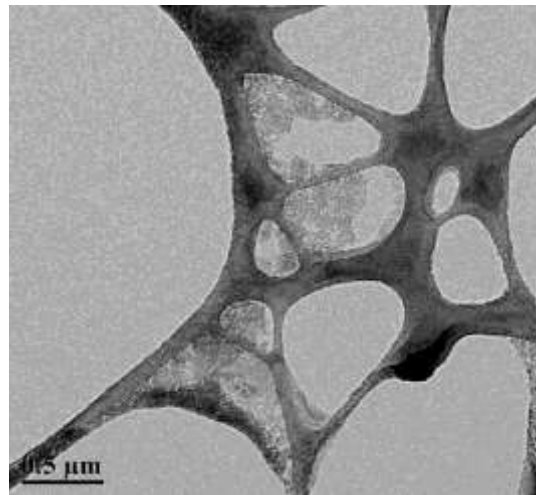
(b)
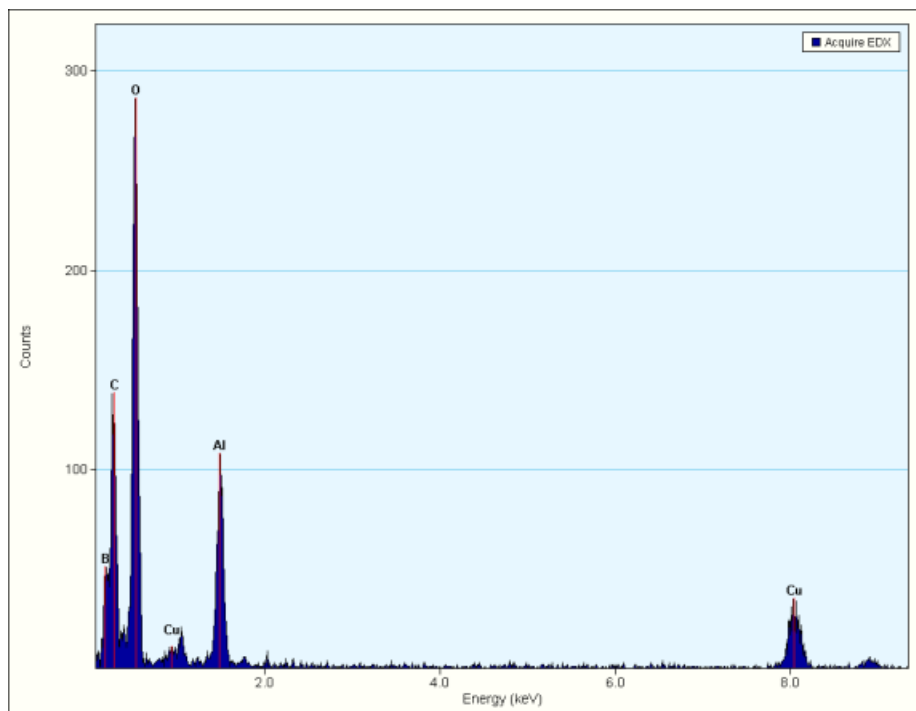
(c)

Figure 18: TEM Analysis - Rapid Cooling (RC) Sample (a) Electron Diffraction Pattern

(b) TEM image (c) EDS Analysis
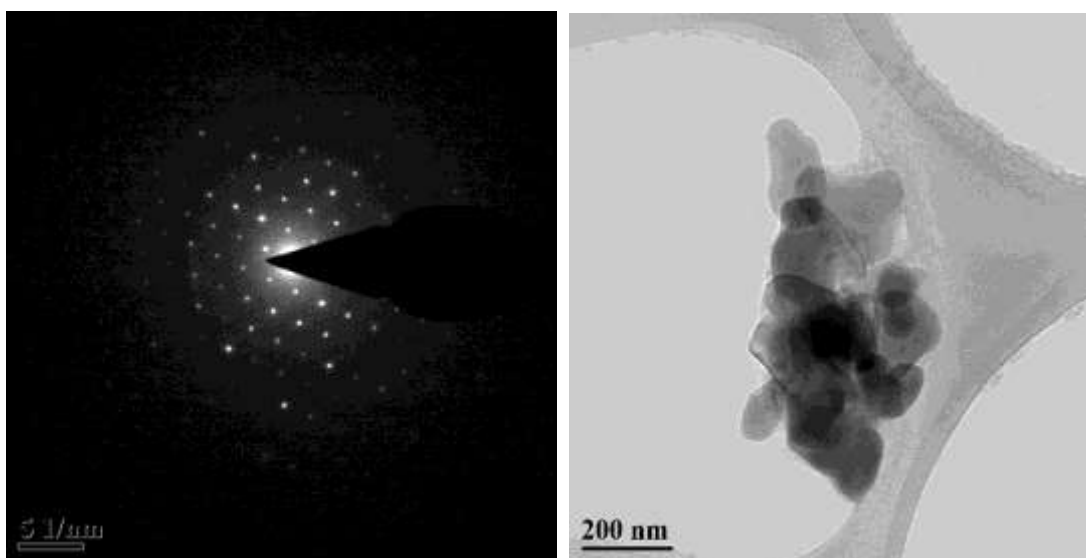
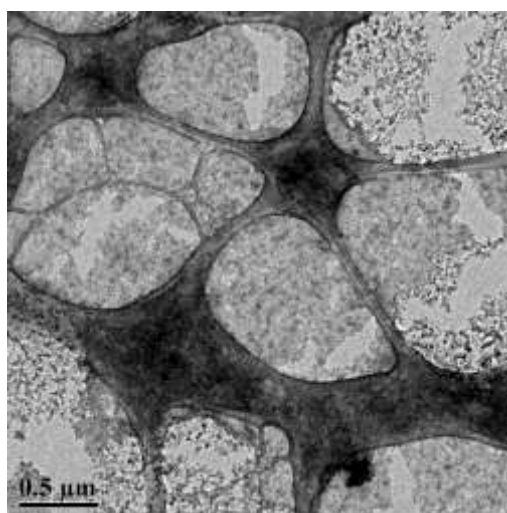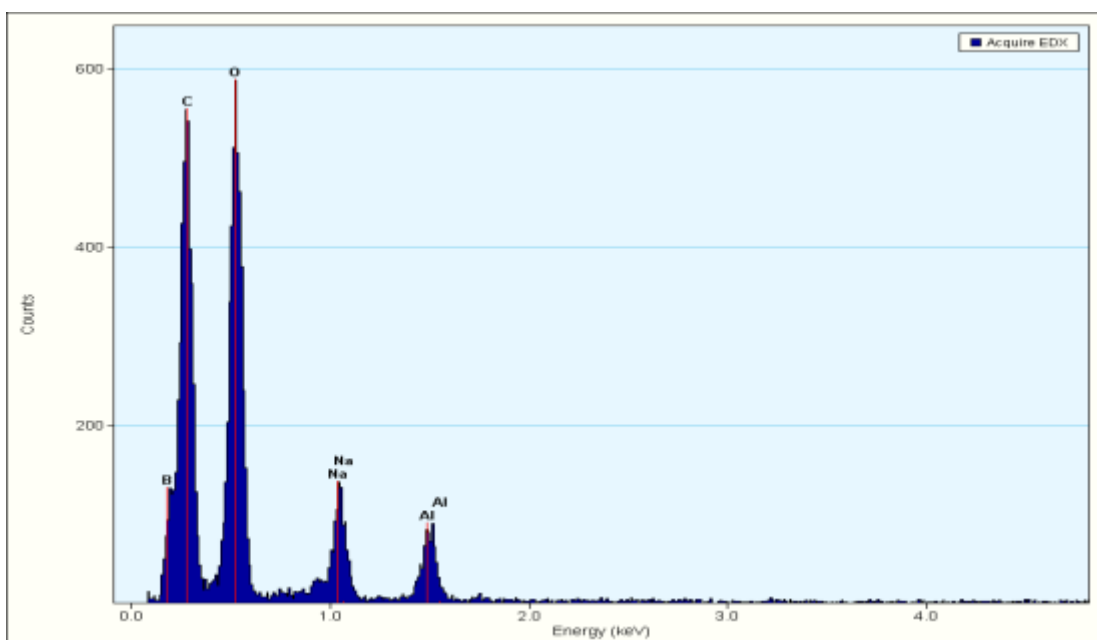(a)   (b)
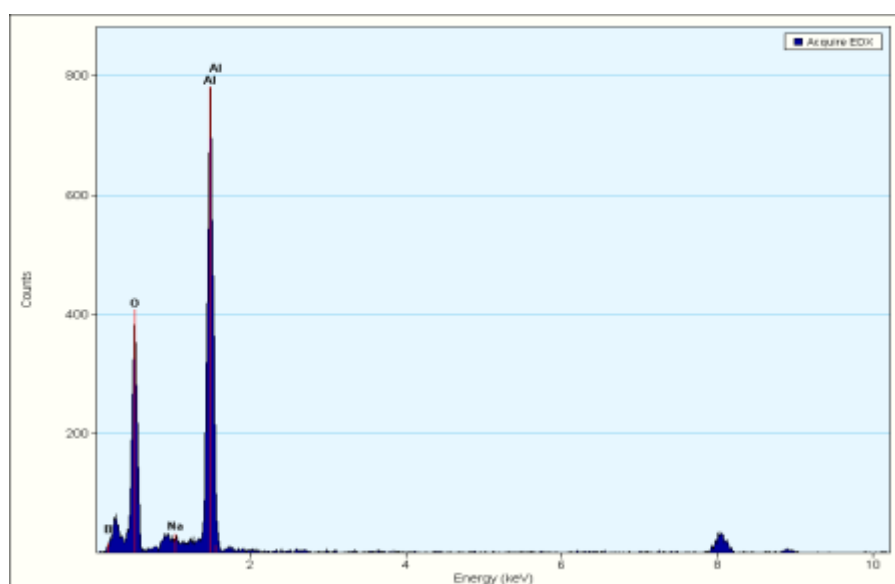
(c)

Figure 19: TEM Analysis - Intermediate Cooling (IC) Sample (a) Electron Diffraction

Pattern (b) TEM image (c) EDS Analysis
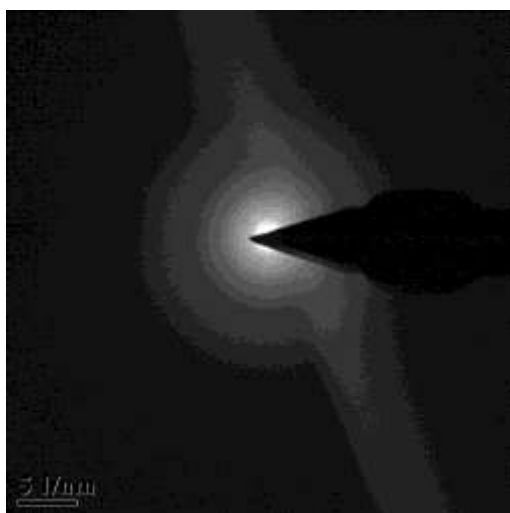
(a)

(b)

(c)

Figure 20: TEM Analysis – Slow Cooling (SC) Sample (a) Electron Diffraction Pattern

(b) TEM image (c) EDS Analysis

EDS cannot detect hydrogen so the exact compositional information cannot be confirmed. However, since the ratio of Al to O is 0.5 for AlOOH and 0.67 for Al_2O_3 it may be plausible to think that the RC may have produced AlOOH compounds and slower cooling rates may have produced two different Al compounds, namely AlOOH compounds (both in amorphous or crystalline structure) Al_2O_3. The O to Al ratio is around 4 for SC compounds indicating the possible formation of boehmite or diaspora both having O to Al ratio of about 2.

It has to be remarked that, due to the low concentration of Al in the samples analyzed, statistical analysis was not conducted for this test. In particular, particles shown in the Figures 18-20 were isolated when performing the scanning and information on the presence of similar particles in the sample analyzed is not reported. The analyses confirmed that the presence of Boron did not affect the measurements since concentrations of boron in the areas analyzed where almost undetectable. It has also to be remarked that the intensity peak of the oxygen may be affected by the inevitable presence of this element in atmospheric composition.
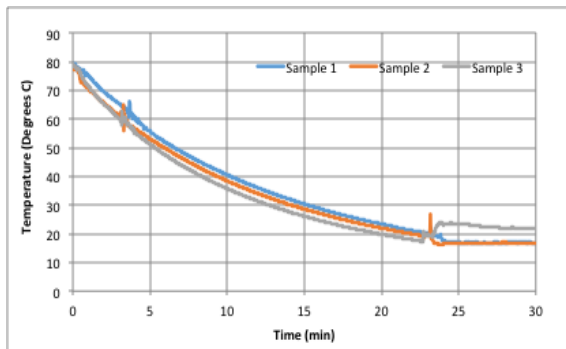
3102/3202

Tests 3102/3202 were completed. Samples were exposed to three different cooling rates and their PSD and turbidity were analyzed. The scope to investigate the combined effect of pH and cooling rate on aluminum precipitate characteristics.
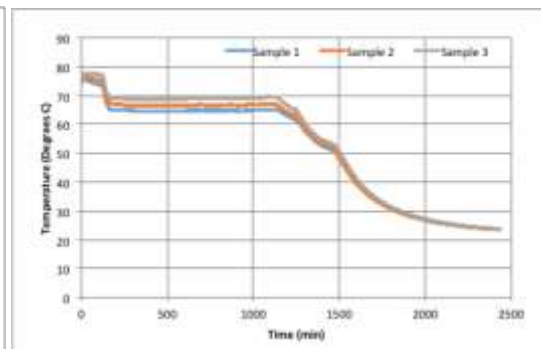
Cooling Rates

Table 12: Cooling rate data for test series 3102/3202

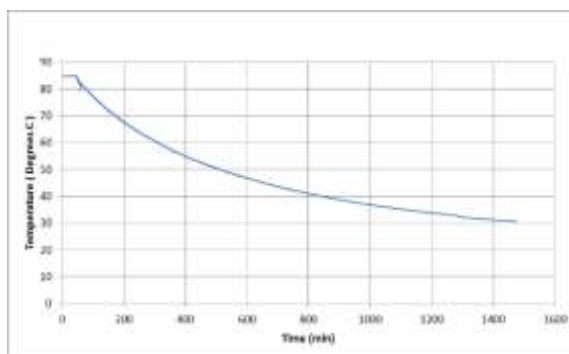| Sample description	Cooling rate (°C/hr.)	Cooling time (minutes)
Rapid Cooled sample (RC)	210	14
Intermediate Cooled sample (IC)	2.42	1,483
Slow Cooled sample (SC)	1.84	1,839

(a)   (b)

Figure 21: Cooling rate graphs for tests series 3102/3202 (a) Rapid Cooling (b) Slow

Cooling (c) Intermediate Cooling

(c)

Figure 21 Continued

ICP Analysis

One sample was taken from the tank at the end of the corrosion period (after Al foil was removed, and prior to cooling) to measure the Al concentration in the solution. The sample was acidified with approximately 0.5mL ACS reagent grade 69% HNO_3 (CAS # 7697-37-2) per 125 mL of sample to prevent any aluminum from precipitating out of solution before the ICP results were obtained. The instrument used to measure the samples is a Perkin Elmer NexIon 300D ICP Coupled Mass Spectrometer. The final ICP measurement for aluminum concentration showed that the concentration in the solution was 69.02 mg/l.

Turbidity Analysis
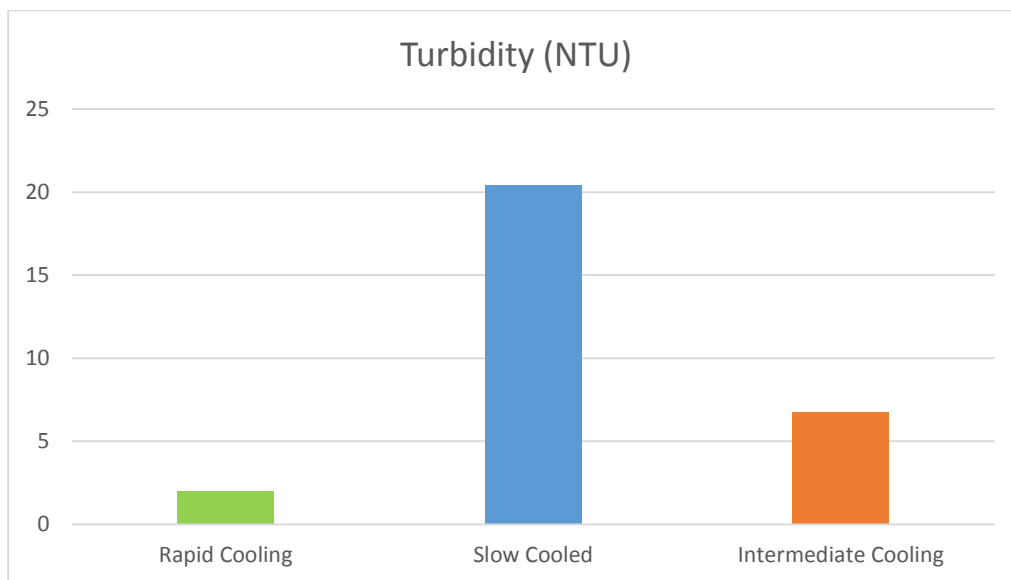
Figure 22: Turbidity analysis for test series 3102/3202.

Based on the cooling rate data, a trend for higher turbidity with slower cooling rates was observed (Fig 22). The slower cooling rates show evidence for a higher turbidity within the solution.

Particle Size

Table 13: Particle size distribution analysis for test series 3102/3202.

Sample Name	Size 1 (nm)	Volume percent of size 1	Standard Deviation (nm)	Size 2	Volume percent of size 2	Standard Deviation (nm)
RC	11.65	99.8%	3.99	-	-	-

Table 13 Continued

Sample Name	Size 1 (nm)	Volume percent of size 1	Standard Deviation (nm)	Size 2	Volume percent of size 2	Standard Deviation (nm)
IC	33.35	88.9%	18.93	4254	8.5%	1235
SC	74.43	90.7%	46.86	-	-	-

Table 13 shows particle size distribution analysis for samples cooled at different cooling rates. The particle size distribution and the turbidity results (Fig 21) were compared and there was an evident trend of increase in particle size and turbidity with a decrease in the cooling rate.

TEM Analysis

Analysis of three samples using the three cooling rates (RC, IC, and SC) were performed with TEM to study precipitate characteristics of interest such as morphology and composition. Different areas were subject to observation and analysis from the samples selected. Figures 23,24,25 summarize the main observations for selected areas of the RC, IC, and SC samples respectively.

The most outstanding feature of samples 3202-IC and 3202-SC (Fig 24 and Fig 25 respectively) is that particles appear to be homogeneous in morphology while the shapes of both samples are somewhat similar to each other. Also, they have an amorphous structure, consisting dominantly of aluminum and oxygen. On the other hand, particles in sample 3202-RC are not homogeneous in morphology,

crystallography, and component elements. Thus, they can be either amorphous or crystalline while they often contain sodium or calcium.

The difference in samples 3202-IC and 3202-SC is the atomic ratio of O to Al, ($\sim$ 6.5 for IC, $\sim$ 4 for SC). The atomic ratios are a lot greater than 1.5 and particles in both samples do not show a typical alumina crystal structure such as alpha or gamma phase. Therefore, the particles in samples 3202-IC and 3202-SC cannot be Al_2O_3. It is not clear, however, that they are boehmite or diaspore either because the atomic ratios are still much higher than 2. Since crystalline structure is seen only in sample 3202-RC the additional elements might play some role in crystalizing the aluminum compound.
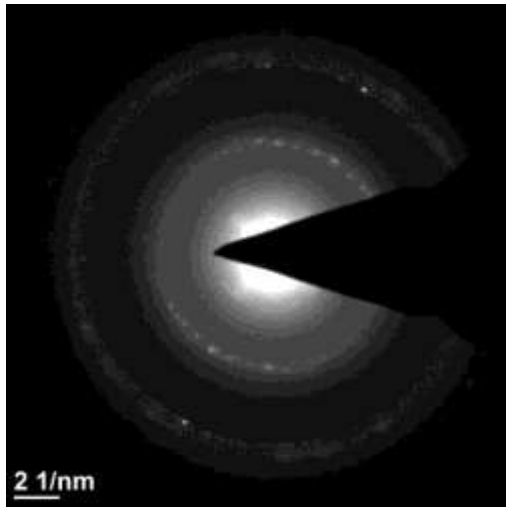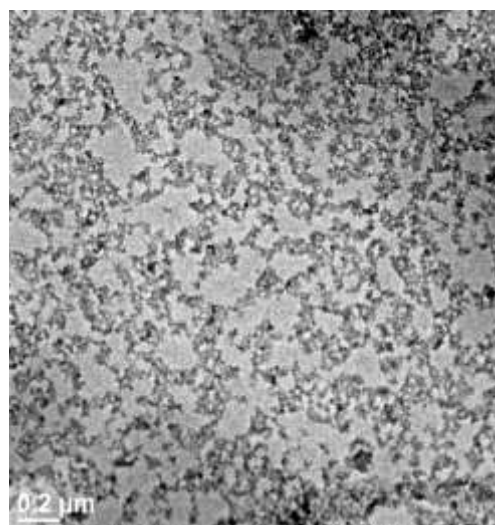
(a)
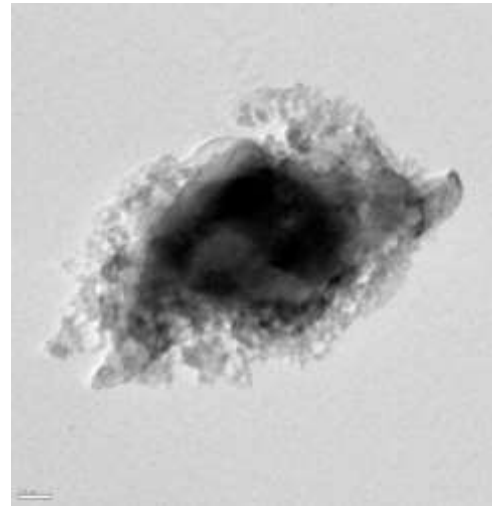
(b)
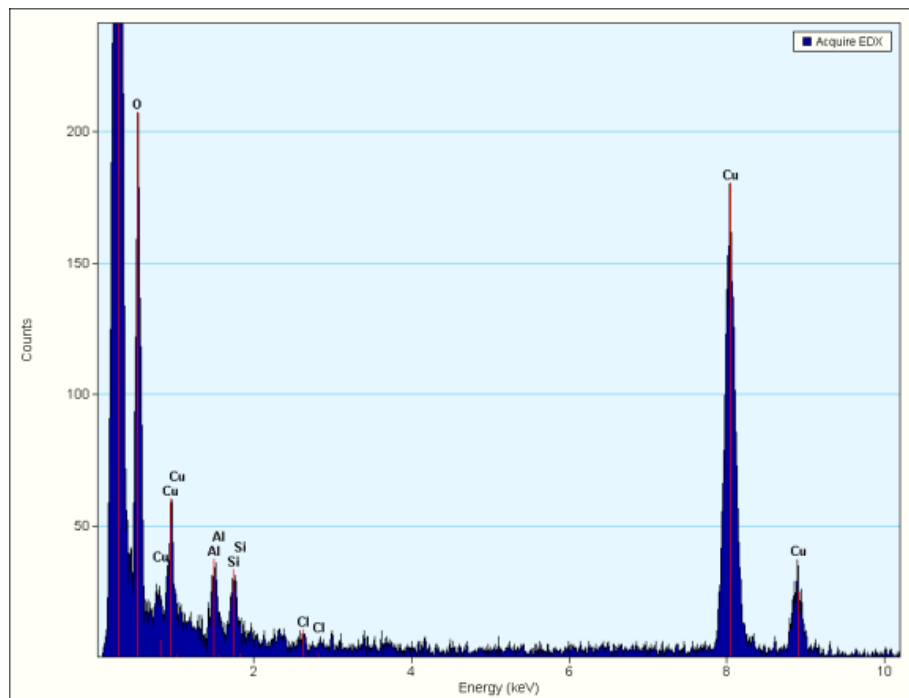
(c)
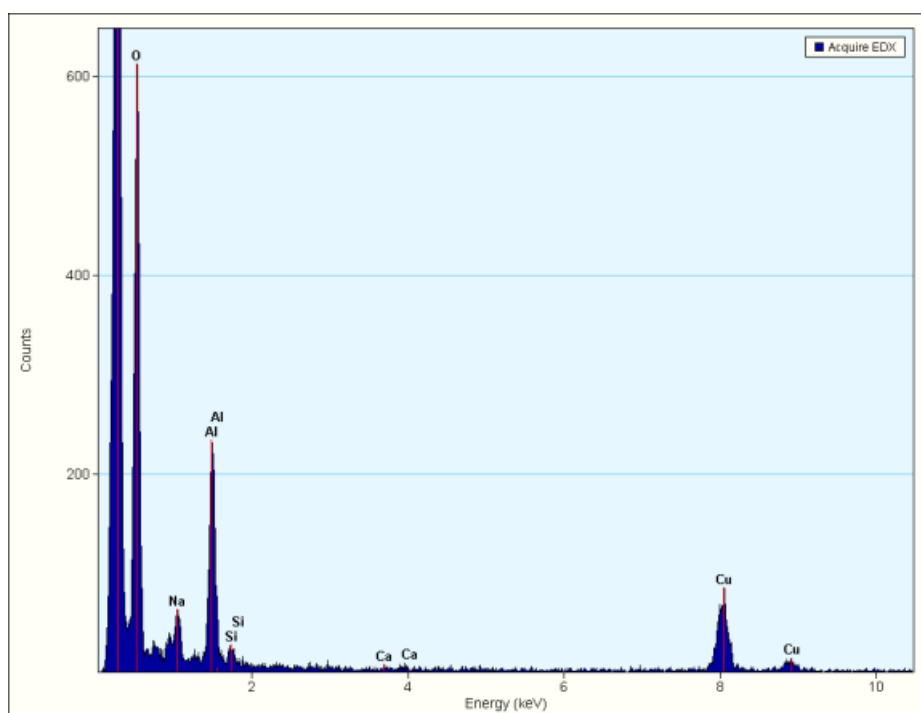
Figure 23: TEM Analysis - Rapid Cooling (RC) Sample (a) Electron Diffraction Pattern

(b) TEM image (c) EDS Analysis
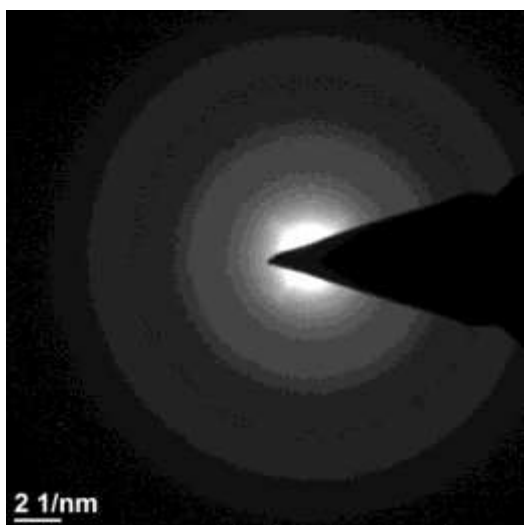
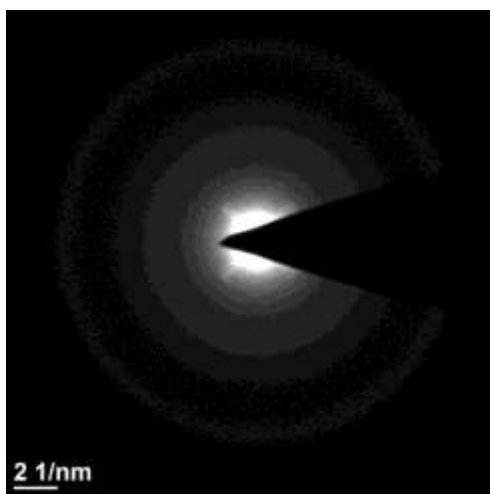(a)   (b)
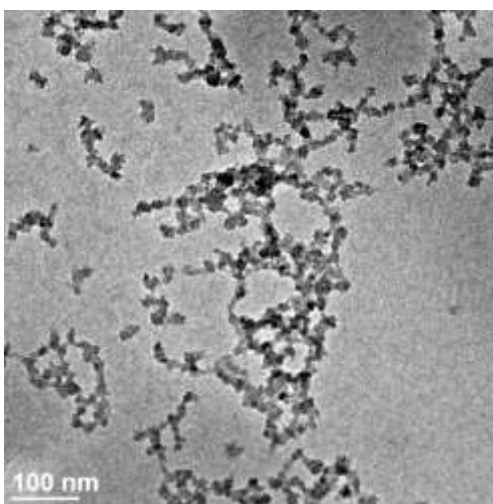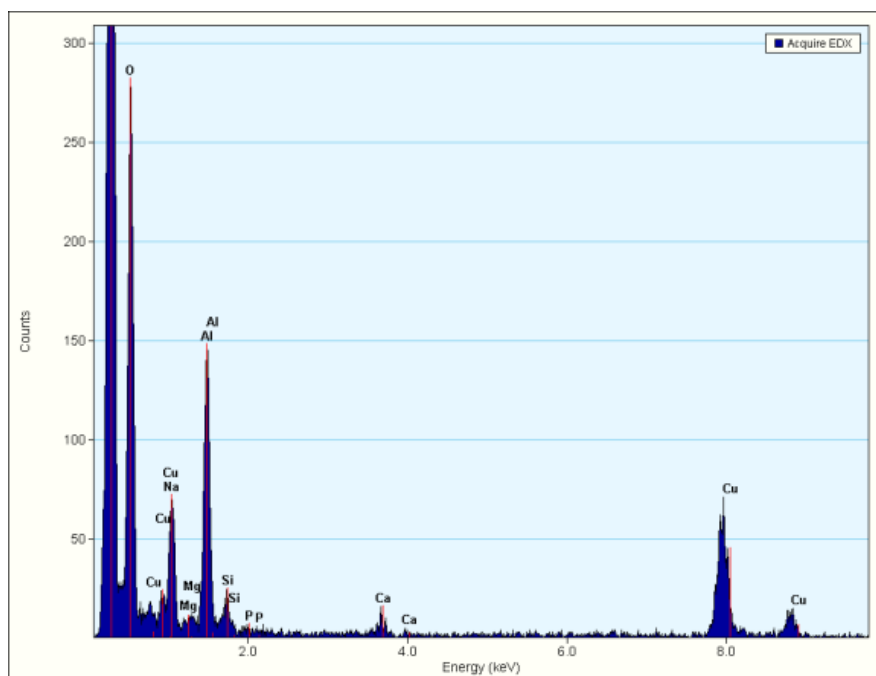

(c)

Figure 24 : TEM Analysis - Intermediate Cooling (IC) Sample (a) Electron Diffraction

Pattern (b) TEM image (c) EDS Analysis

(a)

(b)

(c)

Figure 25: TEM Analysis – Slow Cooling (SC) Sample (a) Electron Diffraction Pattern

(b) TEM image (c) EDS Analysis

It has to be remarked that, due to the low concentration of Al in the samples analyzed, statistical analysis was not conducted for this test. In particular, particles shown in the Figures 22-24 were isolated when performing the scanning and information on the presence of similar particles in the sample analyzed is not reported. The analyses confirmed that the presence of Boron did not affect the measurements since concentrations of boron in the areas analyzed where almost undetectable. It has also to be remarked that the intensity peak of the oxygen may be affected by the inevitable presence of this element in atmospheric composition.

3103/3203

Tests 3103/3203 were completed. Samples were exposed to three different cooling rates and the PSD and turbidity of the samples were analyzed. The scope to investigate the combined effect of pH and cooling rate on aluminum precipitate characteristics.
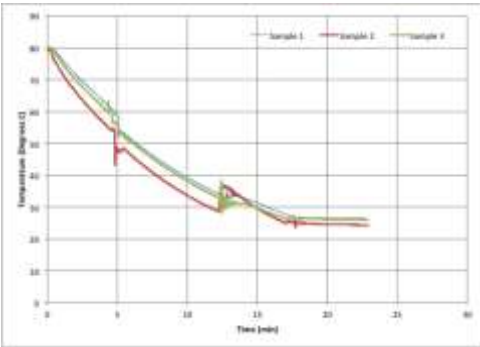
Cooling Rate
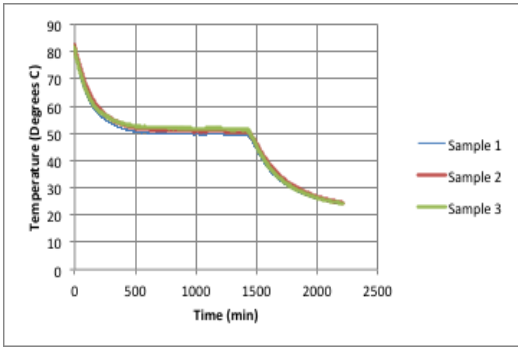
Table 14: Cooling rate data for test series 3103/3203

Sample description	Cooling rate (°C/hr.)	Cooling time (minutes)
Rapid Cooled sample (RC)	192	15.6
Intermediate Cooled sample (IC)	2.63	1,256

Table 14 Continued

Sample description	Cooling rate (°C/hr.)	Cooling time (minutes)
Slow Cooled sample (SC)	1.68	1,786

(a)

(b)
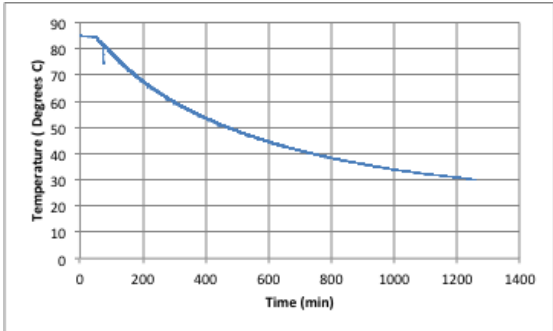
(c)

Figure 26: Cooling rate graphs for tests series 3103/3203 (a) Rapid Cooling (b) Slow

Cooling (c) Intermediate Cooling

ICP Measurements

One sample was taken from the corrosion tank at the end of the corrosion period (after Al foil was removed, and prior to cooling) to measure the Al concentration in the solution. The sample was acidified with approximately 0.5 mL ACS reagent grade 69% HNO_3 (CAS # 7697-37-2) per 125 mL of sample to prevent any aluminum from precipitating out of solution before the ICP results were obtained. The instrument used to measure the samples is a Perkin Elmer NexIon 300D ICP coupled mass spectrometer. The final ICP measurements for aluminum concentration showed that the concentration in the solution was 75.67 mg/L and 74.90 mg/L.
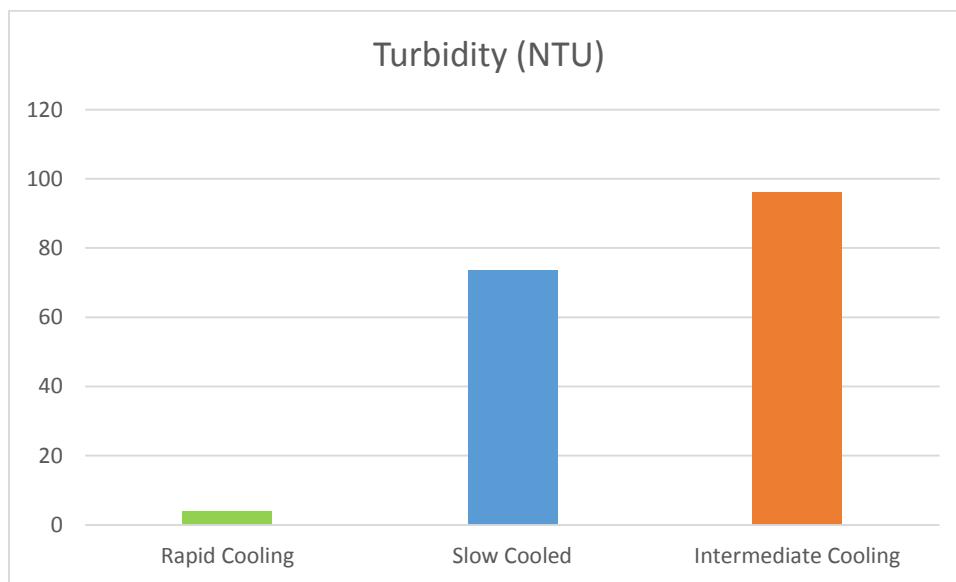
Turbidity Measurements

Figure 27: Turbidity analysis for test series 3103/3203.

Based on the cooling rate data, a trend for higher turbidity with slower cooling rates was observed (Fig 27). Slower cooling rates show evidence for a higher turbidity within the solution. The samples have exhibited no substantial change in turbidity over time thus far so no size measurements have been reproduced.

PSD Distributions

Table 15: Particle size distribution analysis for test series 3103/3203

| **Sample Name**	Size 1 (nm)	Volume percent of size 1	Standard Deviation (nm)	Size 2	Volume percent of size 2	Standard Deviation (nm)
RC	19.12	98.87%	5.81	170.03	1.13%	52.36
IC	48.11	50.1%	12.15	407.1	49.9%	174.6
SC	148.47	56.7%	72.13	227.86	43.3%	95.02

Table 15 shows the particle size distribution at different cooling rates for the experiment at pH 8.2. As seen from Table 11 and Table 13, rapid cooling produced particles that were smaller than particles formed from intermediate or slow cooling. The cooling rates for the slow cooling was not uniform throughout the experimental run period leading to the production of particles of two different sizes.
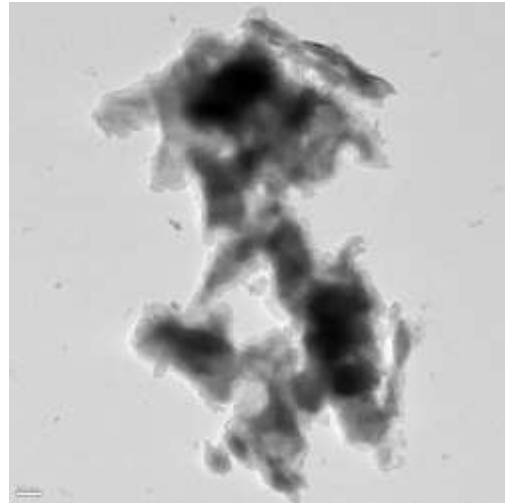
TEM Analysis

Analysis of three samples using the three cooling rates (RC, IC, and SC) were performed with TEM to study precipitate characteristics of interest such as morphology and composition. Different areas were subject to observation and analysis from the

samples selected. Figures 28, 29, 30 summarize the main observations for selected areas of the RC, IC, and SC samples respectively. Sample 3103-IC was found to be similar to IC and RC samples generated during the test 3202 (pH 7.5) both in morphology and crystallography. The atomic ratio of O to Al for this sample ranged between is 2.7 and 4, which is relatively close to 2 for Al-O-OH.

RC and SC samples did not show a sharp Al peak. Measurement of particles in the samples does not suggest a clear indication that they are Al compounds. It is possible to think the unexpected results come from the low concentration of these samples. Since the particles or particle aggregates observed from these samples did not show the Al transition in EDS explicitly, it may be also possible to assume that there is only a very small amount of Al in the samples.
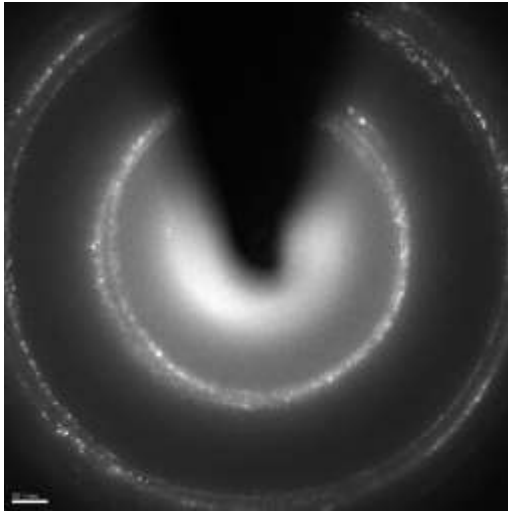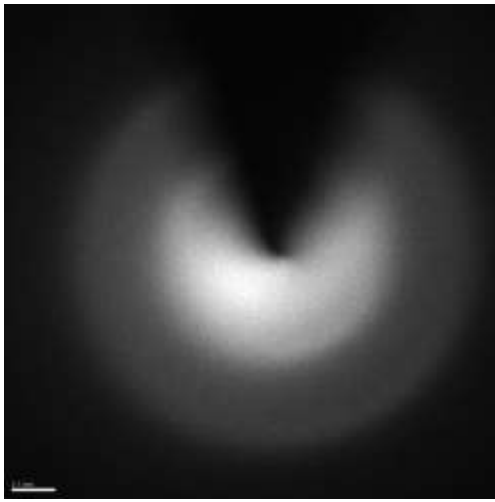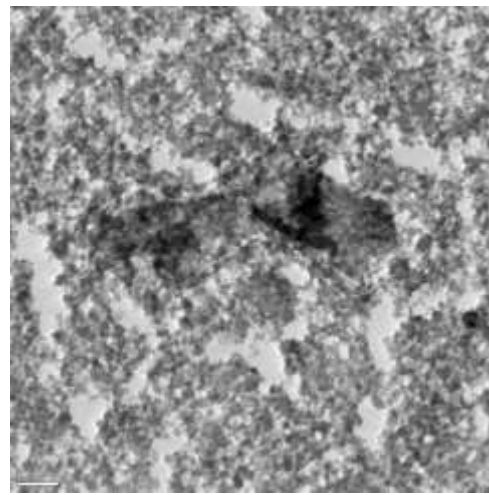
(a)

(b)
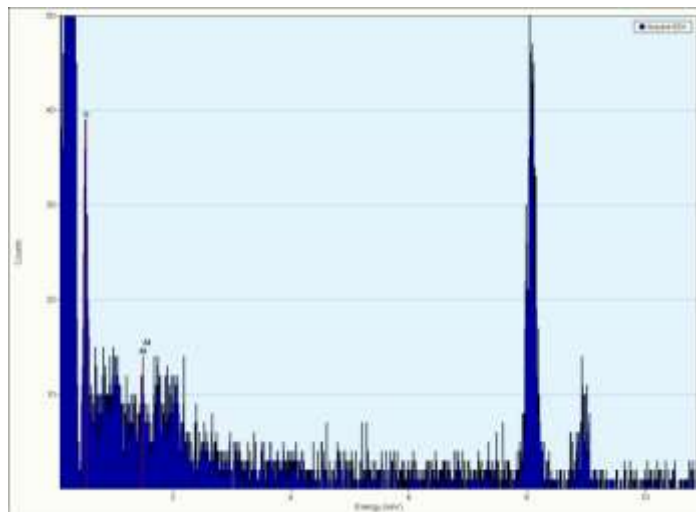
(c)
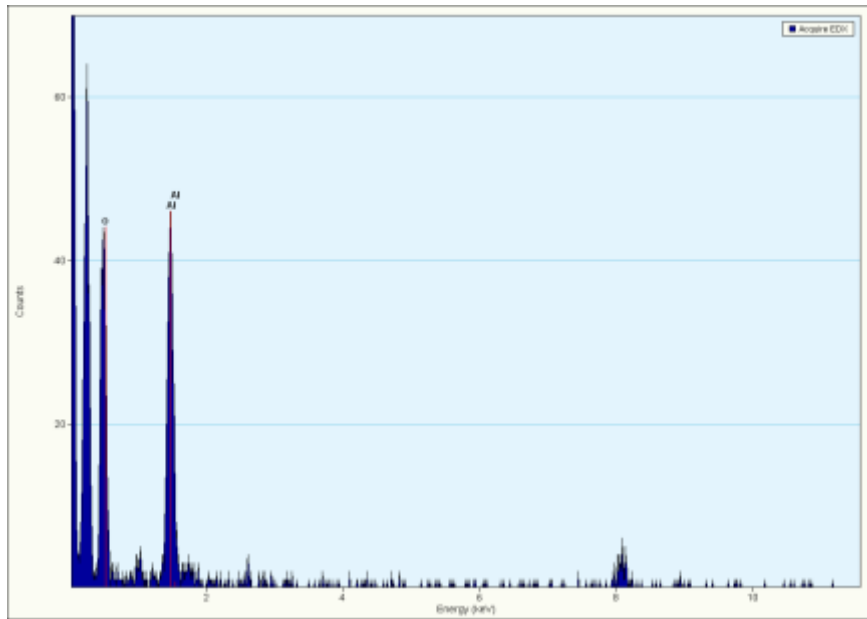
Figure 28 : TEM Analysis - Rapid Cooling (RC) Sample (a) Electron Diffraction Pattern

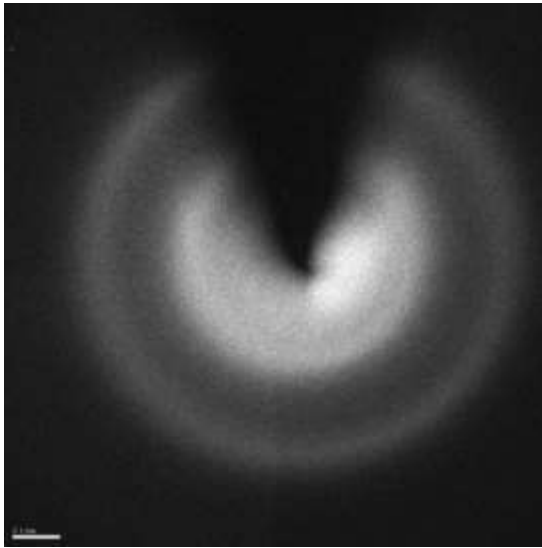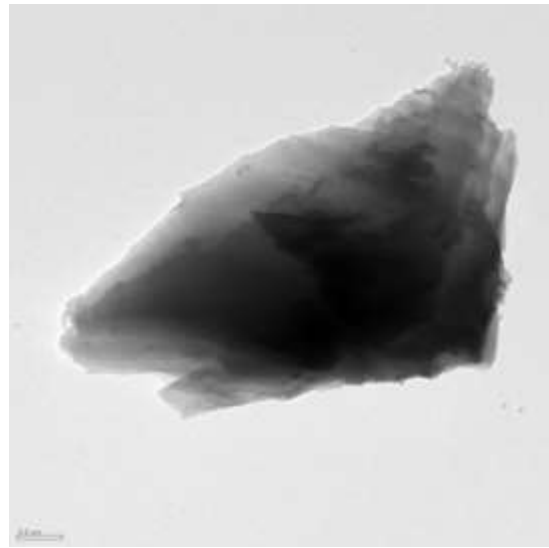(b) TEM image (c) EDS Analysis

(a)

(b)

(c)

Figure 29 : TEM Analysis - Intermediate Cooling (IC) Sample (a) Electron Diffraction

Pattern (b) TEM image (c) EDS Analysis

(a)

(b)
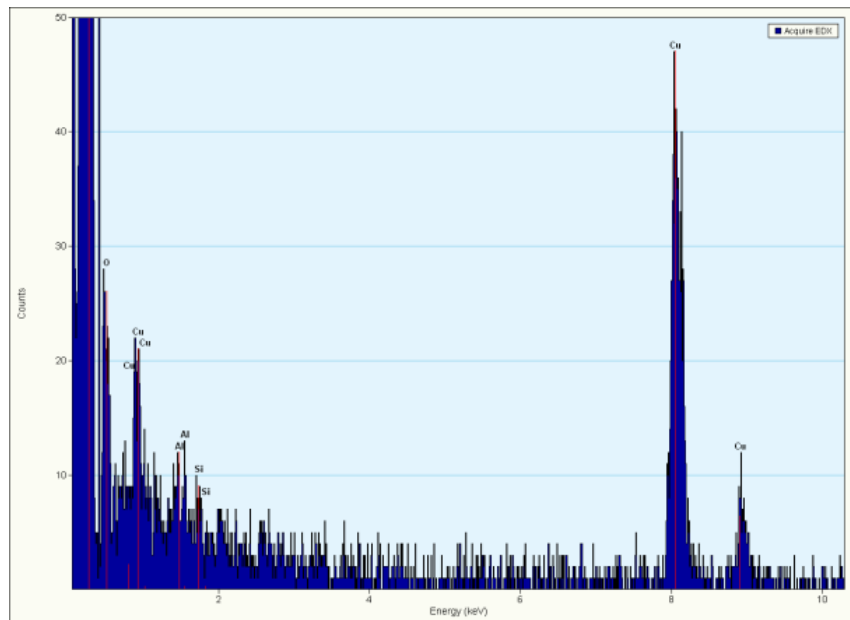
(c)

Figure 30 : TEM Analysis - Slow Cooling (SC) Sample (a) Electron Diffraction Pattern

(b) TEM image (c) EDS Analysis

It has to be remarked that, due to the low concentration of Al in the samples analyzed, statistical analysis was not conducted for this test. The analyses confirmed that the presence of Boron did not affect the measurements since concentrations of boron in the areas analyzed where almost undetectable. It has also to be remarked that the intensity peak of the oxygen may be affected by the inevitable presence of this element in atmospheric composition.

CHAPTER V

CONCLUSION AND FUTURE WORK

5.1 Conclusion

The test facility at Texas A&M helped in creating representative post-LOCA precipitates. An initial bench scale corrosion analysis provided an idea on scaling up the experiment. The process was up-scaled to a 50 gallon tank and the effects of pH, temperature were testing on the concentration, turbidity and morphology of the particles. It was found that pH had a significant effect on the concentration of the particles generated with increase in pH increasing the concentration of aluminum precipitates generated. The rate of cooling decided the size of the particles and also the crystallinity of the generated particles with the increase in cooling rate increasing the size of the particles generated. The rapid cooling rate seemed to generate AlOOH as the precipitate as determined from the EDS, and the particles tend to be non-homogeneous in nature. The intermediate cooling, however, produced particles that were more homogenous and also tend to form other morphological forms of Al_2O_3 apart from Υ-alumina, sometimes forming AlOOH as well. Slow cooling also generated homogenous amorphous particles with an O to Al ratio of around 4 indicating the possible formation of boehmite or diaspore compound. Characterizing these particles can add to the database of effects of pH and temperature on alumina as well as help in creating new surrogates for testing the effects of these particles on the strainers for large scale head loss testing.

5.2 Future Work

Characterizing these particles will help in creation of surrogate salts that have similar morphology as actual corrosion products, and thus can be used for larger scale head loss testing. The surrogates can also be considered as representative post-LOCA particles, and this can help design more accurate head loss testing processes. Further work also involves testing the presence of other metals on the concentration and morphology of alumina particles. A correlation between turbidity and concentration/particle size can also be established for easier analysis and characterization using turbidity data alone.

REFERENCES

Andreychek, T. S. (2005). *Test Plan: Characterization of Chemical and Corrosion Effects Potentially Occurring Inside a PWR Containment Following a LOCA.* Monroeville, PA: Westinghouse Electric Company.

Bahn, C. B., Kasza, K. E., Shack, W. J. et al. (2009a). Evaluation of precipitate used in strainer head loss testing Part I. Chemically generated precipitates. In *Nuclear Engineering and Design, Vol 239* (pp. 2981-2991).

Bahn, C. B., Kasza, K. E., Shack, W. J. et al. (2009b). *Evaluation of WCAP aluminum hydroxide surrogate stability at elevated pH.* Argonne National Laboratory, Argonne, IL.

Bahn, C. B., Kasza, K. E., Shack, W. J. (2009c). *Technical Letter Report on Evaluation of Head Loss by Products of Aluminum Alloy Corrosion.* Argonne National Laboratory, Argonne, IL

Bahn, C. B., Kasza, K. E., Shack, W. J. et al. (2011a). Evaluation of precipitates used in strainer head loss testing Part II. Precipitates by in-situ aluminum alloy corrosion In *Nuclear Engineering and Design, Vol 241* (pp. 1926-1936).

Bahn, C. B., Kasza, K. E., Shack, W. J. et al.(2011b). Evaluation of precipitates used in strainer head loss testing: Part III. Long-term aluminum hydroxide precipitate tests in borated water. In *Nuclear Engineering and Design Vol.241* (pp. 1914-1925).

Borchardt, R. W. (2012). *Closure Options for Generic Safety Issue - 191, Assessment of Debris Accumulation on Pressurized-Water Reactor Sump Performance*, Document No. SECY-12-0093, US Nuclear Regulatory Commission, Washington, DC

Chen, A., Zhu, W., Chen, X. et al. (2014). *Decomposition of sodium zincate in alkaline solution by dilution.* Hydrometallurgy, Vol. 149 (pp.82-86)

Dallman, J., Letellier, B., Garcia, J. et al. (2006). *Integrated Chemical Effects Test Project: Consolidated Data Report.* New Mexico: Los Alamos National Labaratory, NM

Hirano, M. , & Kato,E. (1999). *Hydrothermal synthesis of nanocrystalline cerium(IV) oxide powders. Journal of the American Ceramic Society*, *82*(3), 786-788.

Howe, K. J., & Leavitt, J. J. (2012). *CHLE Tank Test Results for Blended and NEI Fiber Beds with Aluminum Addition (CHLE-010)*, Rev 3, University of New Mexico, Albequerque, NM

Hu, X., & Yu, J. C. (2008*). Continuous Aspect-Ratio Tuning and Fine Shape Control of Monodisperse α-Fe2O3 Nanocrystals by a Programmed Microwave–Hydrothermal Method. *Advanced Functional Materials*, *18*(6), 880-887

Johns, R. C., Letellier, B. C., Howe, K. J. et al. (2005). *Small-Scale Experiment: Effects of Chemical Reactions on Debris-Bed Head Loss.* (NUREG/CR-6868) US Nuclear Regulatory Commission, Washington, DC

Kim, S. J., & Howe, K. J.. (2013). *CHLE-019 Test Results for Chemical Effect Tests Stimulating Corrosion and Precipitation.* (T3 & T4). University of New Mexico, Albuquerque,NM

Klasky, M., Zhang, J., Ding, M. et al. (2006). *Aluminum Chemistry in Prototypical Post-LOCA PWR Containment Environment.* (NUREG/CR-6915) Nuclear Regulatory Commission, Washington, DC

Lane, A. E., Andreychek, T. S., Byers, W. A. et al. (2006). WCAP-16530-NP-A: Evaluation of Post-Accident Chemical Effects in Containment Sump Fluids to Support GSI-191.*Westinghouse Electric Company, Pittsburgh, PA*.

Leavitt, J. J., & Howe, K. J. (2012). . CHLE-012: T1 MBLOCA Test Report, Rev. 4. University of NewMexico, Albuquerque, NM.

Leavitt, J. J., & Fullerton, C. (2013). *Unpublished aluminum and silicon NMR results.* University of New Mexico, Albuquerque, NM.

Muschol, M., & Rosenberger, F.,(1997). Liquid–liquid phase separation in supersaturated lysozyme solutions and associated precipitate formation/crystallization. *The Journal of chemical physics*, *107*(6), 1953-1962.

Saito, G. ,Hosokai, S., Tsubota, M. et al. (2012). *Influence of Solution Temperature and Surfactants on Morphologies. Crystal Growth & Design*, *12*(5), 2455-2459.

Xuan, W. W., Whitty, K. J., Guan, Q. L. et al. (2014). Influence of isothermal temperature and cooling rates on crystallization characteristics of a synthetic coal slag. *Fuel*, *137*, 193-199.

Zhou, Q., Zhao, H. L., Shao, Z. C. et al. (2012). Influence of Parameters on Alumina Particles Size and Morphology. In *Advanced Materials Research* (Vol. 382, pp. 336-339). Trans Tech Publications.